CA2ALRC
91L03
c.v

LEGISLATURE LIBRARY
FEB20 1992
EDMONTON

ALBERTA RESEARCH COUNCIL

Environmental Research and Engineering

WINTER TRACER DYE STUDIES ON THE NORTH SASKATCHEWAN RIVER, EDMONTON TO SASKATCHEWAN BORDER

Open File Report 1991-3

by

G. Van Der Vinne

Environmental Research and Engineering Department
Alberta Research Council

for

Alberta Environment

Edmonton, Alberta
Report No. SWE-04
Jan 1991

93-02119/

ABSTRACT

Two tracer dye tests were carried out on the North Saskatchewan River to define the hydraulic and mixing characteristics of the river reach between Edmonton and the Saskatchewan border for mid-to-late winter ice conditions. Discharges during the tests ranged from 108 m^3/s to 153 m^3/s. Ice cover thicknesses varied between 0.3 m and 0.8 m although frazil accumulations approaching 2 m were found in some sections. The mean water velocities calculated from the travel time of the peak dye concentration was 0.65 m/s in the open water reach between Edmonton and Fort Saskatchewan, 0.55 m/s in the ice covered reach between Fort Saskatchewan and Shandro and 0.49 m/s in the ice covered reach between Shandro and the Saskatchewan border. Composite hydraulic roughnesses varied between 0.016 to 0.038. These composite roughnesses can be used to extrapolate velocities at other discharges provided that the ice characteristics do not change significantly.

Both linear and Fickian dispersion occurred in the test reaches. The linear dispersion parameter was found to be 0.00612 for the Edmonton injection and 0.00429 for the Shandro injection. These values are lower than the values measured on other ice covered rivers but this is due to the low values of hydraulic roughness found in these river reaches. The Fickian dispersion coefficient was found to be 344 m^2/s for the upper test reach and 291 m^2/s for the lower test reach. These values are consistent with values reported in the literature for channels of similar width and roughness even with the presence of the ice cover. The location of the transition between linear and Fickian dispersion was found to depend on the position and number of injection points.

Both the linear and Fickian dispersion models predicted much more symmetrical distributions than were actually observed. The models accurately predict dispersion in uniform channels but the variations in geometry in natural rivers causes additional mixing which the models do not predict.

ACKNOWLEDGMENTS

The work reported herein resulted from a joint venture undertaken by the Environmental Protection Service of Alberta Environment and the Surface Water Engineering Group of the Environmental Research and Engineering Department, Alberta Research Council.

Numerous individuals contributed to and provided support for this project. J. Thompson, B. Trevor, P. Mostert and R. Bilyk of the Alberta Research Council performed the field work. S. Procyk processed and plotted much of the data. The Water Survey Section of Alberta Environment provided discharge estimates. S. Lovell of the Department of Civil Engineering, University of Alberta made the U of A fluorometer available for use in this study.

The results achieved were very much a function of the skills developed over many years of involvement with the ongoing Alberta Cooperative Program in Transportation and Surface Water Engineering, participants of which are the Alberta Research Council, Alberta Transportation and Utilities, Alberta Environment, and the Department of Civil Engineering, University of Alberta.

TABLE OF CONTENTS

	Page
Abstract	i
Acknowledgments	ii
Table of Contents	iii
List of Figures	iv
List of Tables	v
1.0 INTRODUCTION	1
1.1 Background	1
1.2 Objectives	2
2.0 FIELD INVESTIGATION	3
2.1 Study Reaches	3
2.2 Methodology	3
2.2.1 Injection	3
2.2.2 Sampling	7
2.2.3 Calibration and Data Reduction	8
2.3 Discharge Measurements	9
3.0 TRAVEL TIME ANALYSIS	11
3.1 Channel Hydraulics	11
3.2 Generalized Travel Times	16

TABLE OF CONTENTS (Continued)

Page

4.0 LONGITUDINAL DISPERSION ANALYSIS 20
4.1 Reach-average Hydraulic Characteristics 20
4.2 Mixing Zones 21
4.2.1 Vertical Mixing 21
4.2.2 Transverse Mixing 22
4.2.3 Linear Dispersion 25
4.2.4 Fickian Dispersion 27
4.3 Dispersion Parameters 28
4.4 Dispersion Model Predictions 31
4.4.1 Linear Dispersion 31
4.4.2 Fickian Dispersion 34

5.0 SUMMARY 37

6.0 REFERENCES 39

APPENDIX A
Dye Concentration Measurements 41

LIST OF FIGURES

		Page
Figure 1a-b	Location plan	4 (in pocket)
Figure 2a-b	Growth of travel times with distance from injection	13
Figure 3	Relationships between mean velocity and discharge per unit width for the North Saskatchewan River under an ice cover	18
Figure 4	Definition sketch for variables describing time-concentration distributions	27
Figure 5	Variation of half-duration with time-to-peak from injection	30
Figure 6	Variation of β for both open water and ice covered conditions (Beltaos, 1978b)	30
Figure 7	Increase in variance with distance from injection ..	32
Figure 8	Variation of dimensionless dispersion coefficients (Beltaos, 1978b)	32
Figure 9	Comparison of measured time-concentration distributions with those predicted by the linear dispersion model	33
Figure 10	Variation in mass recovery ratio with distance from injection	34

LIST OF TABLES

		Page
Table 1	Summary of field program	6
Table 2	Summary of adopted subreach-averaged discharges	10
Table 3	Subreach average travel times	12
Table 4	Summary of the average hydraulic characteristics in late winter for each subreach	15
Table 5	Reach-average hydraulic characteristics	20
Table 6	Summary of mixing lengths for single centerline injections	21
Table 7	Position parameters for various fractions of cumulative discharge across a section and 95% complete mixing	23
Table 8	Transverse mixing lengths for multiple injections	24
Table 9	Summary of cross-section average time-concentration distribution variables	29
Table 10	Summary of dispersion parameters	29

1.0 INTRODUCTION

1.1 Background

Increased awareness of environmental issues has prompted a reevaluation of the impacts of effluent discharges on the water quality of many Alberta rivers. Water quality modeling techniques are now being used to reassess the impacts of effluents from existing sources as well as to assess the potential impacts of effluents from new sources. These models provide a better understanding of the effects of effluents on river water quality; however, the models can only be used confidently if the hydraulic and mixing characteristics of the rivers are known.

The most critical conditions for water quality in rivers in northern Alberta usually occur during the winter period. In most of these rivers the lowest flows occur during the winter. These low flows reduce the effluent assimilation capacity of the rivers. As well, the ice covers which exist on these rivers during the winter block the reabsorption of oxygen, thus intensifying the effects of oxygen consumption by some effluents. Unfortunately, there is a distinct lack of information on the hydraulic and mixing characteristics for these low flow ice-covered conditions.

Effluent discharges from the Edmonton area, such as the sewage treatment plant, are being reassessed using the water quality models. One of the first steps in this assessment process is to determine the hydraulic and mixing characteristics of the river system downstream from the effluent outfall during the critical low flow winter period. To this end, the Alberta Research Council was requested by Alberta Environment to conduct tracer dye studies on the North Saskatchewan River between Edmonton and the Saskatchewan border in March of 1990 to measure travel times and to determine the longitudinal dispersion characteristics in this river reach.

1.2 Objectives

This report addresses the objectives of the tracer dye studies conducted on the North Saskatchewan River in March, 1990. These objectives are to:

1. determine the travel times relative to the hydraulic characteristics to extrapolate travel times over a range of possible discharges encountered under an ice cover, and

2. evaluate the longitudinal dispersion characteristics relative to the hydraulic characteristics.

2.0 FIELD INVESTIGATIONS

2.1 Study Reaches

The 336.3 km length of the North Saskatchewan River between Edmonton and the Saskatchewan border was divided into two reaches for which separate dye tests were carried out. The length of the upstream reach was 198.1 km while the length of the downstream reach was 189.6 km. The reaches overlapped for 51.4 km between Shandro and Duvernay to compare the velocity measurements at the beginning and end of a test. These reaches were also chosen so that each dye test would be approximately the same duration.

Figure 1a-b illustrates the entire length of the river between Edmonton and the Saskatchewan border and indicates the pertinent river distances (from the mouth), the two study reaches, locations where dye was injected, and the sample sites. Table 1 summarizes some of this information. The dye was always injected at the upstream end of each reach and concentrations were measured at six locations downstream. The subreaches varied in length from 20 km to 50 km depending on the availability of access. Dye injections proceeded from downstream to upstream to eliminate background interference from residual dye remaining from upstream tests.

2.2 Methodology

2.2.1 Injection

For each dye test, a predetermined volume of 20% Rhodamine WT dye was mixed with an equal volume of methyl alcohol. The methyl alcohol was used to adjust the specific gravity of the dye mixture to that of water. Multiple injection points in the cross-section were used at both injection sites to reduce the initial concentrations and reduce the distance needed to complete the transverse mixing process. At injection, the flow width was determined and the injection points spaced evenly across the channel. Different procedures were used to inject the dye

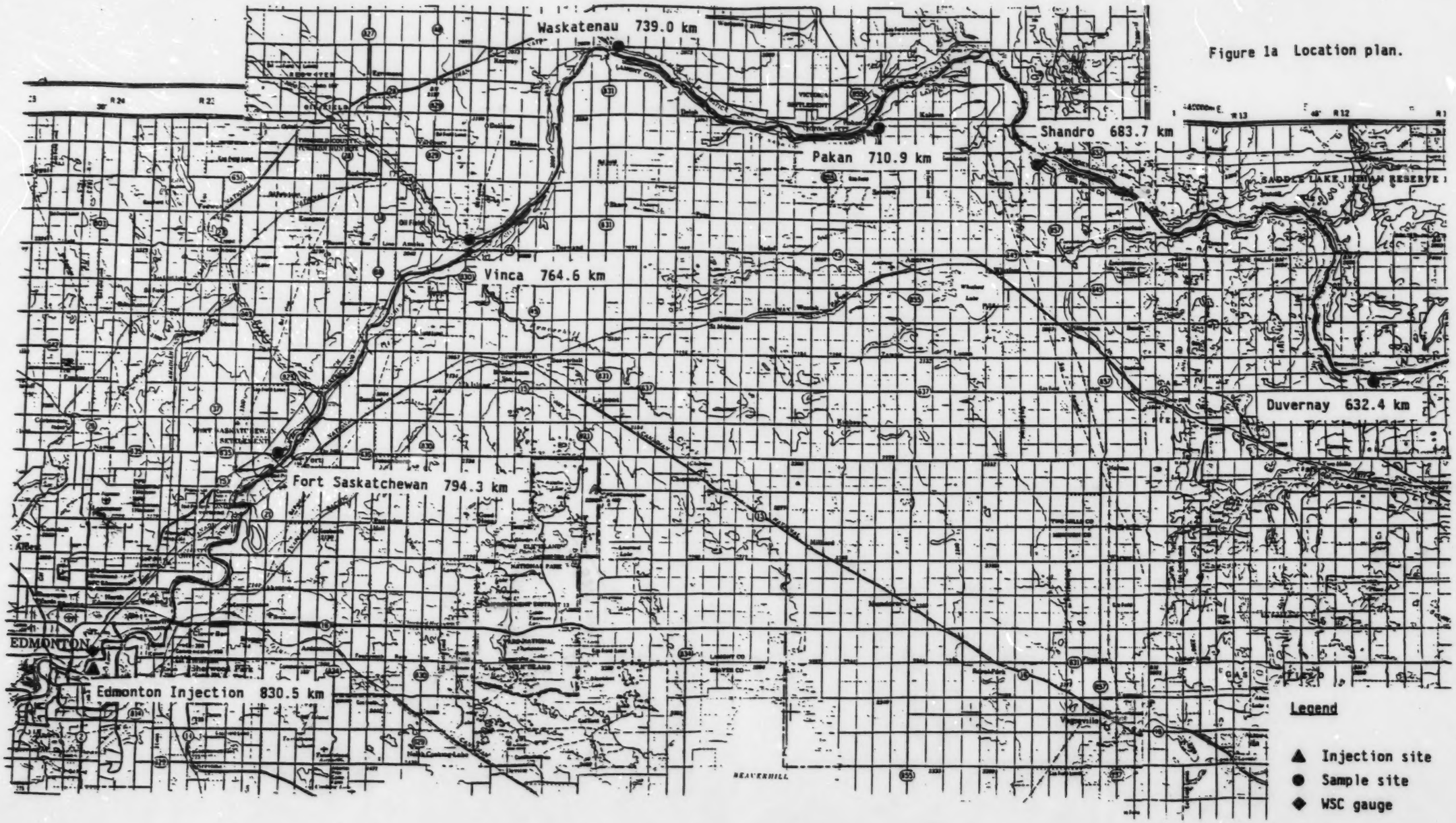

Figure 1a Location plan.

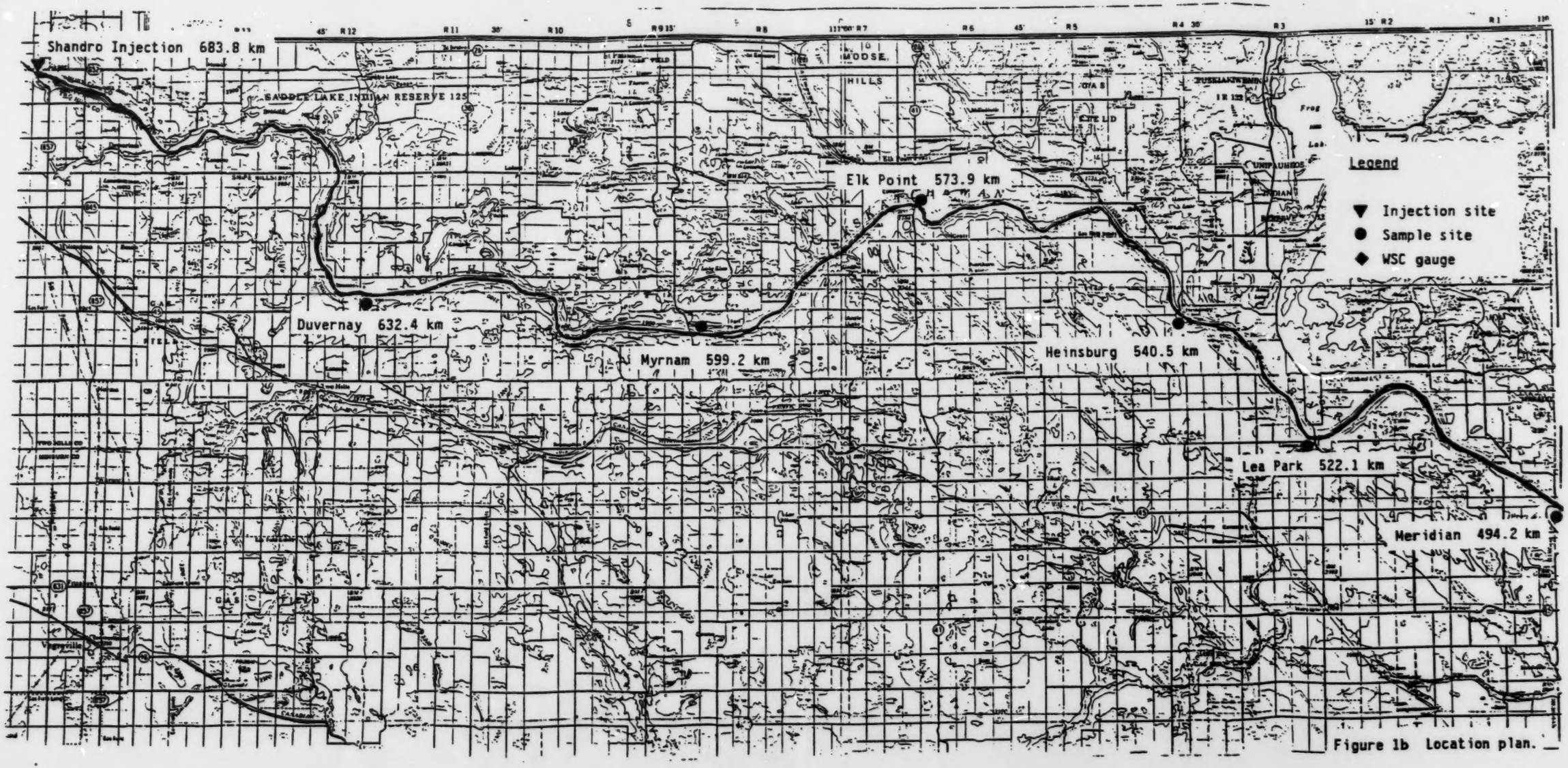

Figure 1b Location plan.

Table 1 Summary of field program.

Reach	Length (km)	Date 1990	Number of Sample Sites	Duration of Test (hours)	Dye Volume (liters)
Shandro - Meridian	189.6	Mar.06-Mar.12	6	132	67.2
Edmonton - Duvernay	198.1	Mar.15-Mar.20	6	123	35.0

into the flow because the river was ice-covered at one site but ice free at the other site.

At the injection site 100 m downstream of the Shandro bridge the river was ice covered so a number of 20 cm diameter holes were augered through the ice to define the width of flow. The two injection holes were selected to divide the channel width into equal segments. Once the injection points were chosen, another series of holes were augured upstream to serve as a water supply to flush the injection apparatus. The injection apparatus consisted of two 1.5 m lengths of 8 cm diameter ABS pipe.

The injection apparatus was lowered into the holes such that the outlets were located in the center of the flow, midway between the bed and the bottom of the ice cover. If a longer length of pipe was required to achieve the desired injection configuration, a 1 m long section could be added to the original length of pipe by a friction coupling. Once the injection apparatus was properly positioned, it was held in place against the ice by a tripod located on the ice surface. The pre-mixed dye was then simply poured into the pipe via a funnel, followed immediately by 20 to 40 L of clean river water to ensure all the dye was removed from the ABS pipe and from the container holding the dye.

The Edmonton injection was done from the Cloverdale pedestrian bridge just downstream of the Low Level bridge. Approximately one-third

of the channel, on the inside of the bend, was blocked by ice so the three injection points were selected to divide the open water portion of the channel into equal segments. The injection was done by using ropes to lower three buckets, each with one-third of the dye, to points just above the water surface. Another set of ropes attached to the bottoms of the buckets were then used to invert the buckets, pouring the dye into the river. The buckets were then immediately dropped into the river to wash away any remaining dye. This procedure produces a surface injection; however, the momentum of the dye causes it to mix well with the water rather than float on the surface.

2.2.2 Sampling

The sampling sites were established at locations where access was available. Following injection at the upstream end of the river reach being characterized, two crews of two persons followed the dye cloud downstream, each of the crews sampling at alternating sites. At each site, a number of 20 cm diameter holes were augured through the ice to establish the flow depth and the ice thickness. The water level was referenced to benchmarks so that water surface slope profiles could be established.

The dye cloud was sampled over three holes across the channel. The centerline sampling location was established in the main part of the flow and two secondary sampling holes were established midway between the centerline sampling hole and both the left and right banks. Sufficient samples were taken at each of the sampling sites to completely characterize the dye cloud. Two or more samples were taken to establish background fluorescence levels and at least 20 samples were taken over the duration of the dye cloud. Depending on the duration of the dye cloud the interval between samples varied between 5 minutes and 2 hours. The secondary sample sites were established to assess the extent of lateral mixing and to improve the estimates of the total volume of dye passing the sampling site.

As mentioned earlier, the entire dye cloud was measured as

completely as possible. Special care was taken to define the time of first rise and the time of peak. Generally, the frequency of sampling was increased during those two periods. On the falling limb of the concentration curve, sampling was continued until it was judged that the fluorescence was reduced to 20% of the peak and that the tail of the curve could be confidently extrapolated. In some cases, however, the tails of the dye cloud were cut short in order to give sufficient time to go to the next sampling site.

As soon as the samples were collected, they were transported to the mobile laboratory which each crew had at its disposal. The samples were maintained at temperatures of about 0 - 2°C (very nearly that of the river) and immediately run through the Turner Designs Model 10 fluorometer and the results recorded. Where the scales on the fluorometer overlapped, readings were taken on both scales to ensure consistency over the range of the two scales of the fluorometer.

2.2.3 Calibration and Data Reduction

Two fluorometers were used during the field study - the ARC Turner Designs Model 10 field unit and the U of A Turner Designs Model 10 rack mounted unit. Each was kept with the same crew for the duration of the entire campaign. Prior to the field work, a set of standards was prepared and both instruments were calibrated at 20°C for the set of standards over a number of scales. After the field work, the instruments were recalibrated both at 20°C for a number of standards over a number of scales, and at 0°C for two standards over the two most used ranges. There was essentially no difference between the pre- and post-field work calibrations.

A simple least squares linear relationship was established for each scale and the fluorescent values recorded in the field were transformed into true fluorescent values, assuming the samples were collected at 20°C. The final adjustment was made to compensate for temperature. Each value was multiplied by 0.62, the ratio of fluorescence between 20°C and 0°C. The data was then plotted and the pertinent character-

istics computed.

2.3 Discharge Measurements

Discharge measurements necessary to characterize the hydraulic conditions of each of the reaches were made by the Water Survey Section of Alberta Environment and the Water Survey of Canada. Three discharge measurements were generally made in each test reach. The first measurement was made as close as possible to the time and location of the injection, the second measurement was made at a sample site near the midpoint of the reach, and the third measurement was made at the end of the reach near the last sample site. Measurements were also made on major tributaries at the appropriate times.

Discharges at each of the sample sites had diurnal fluctuations due to the operation of a hydroelectric plant upstream of Edmonton. Water levels at most sample sites were monitored every two hours so that the fluctuations could be matched with those from Water Survey of Canada water level gauges at Edmonton and Deer Creek in Saskatchewan. Fluctuations in discharge were estimated from winter stage-discharge curves for these sites. Discharges used in the following analysis were the estimated average discharges for the periods of interest. Table 2 summarizes the adopted discharges used in the travel time analysis.

Table 2 Summary of adopted reach-averaged discharges.

Reach	Date	Discharge (m^3/s)
Edmonton Injection		
Edmonton - Ft. Saskatchewan	Mar. 15 - 16	129
Ft. Saskatchewan - Vinca	Mar. 16	108
Vinca - Waskatenau	Mar. 16 - 17	115
Waskatenau - Pakan	Mar. 17	145
Pakan - Shandro	Mar. 17 - 18	132
Shandro - Duvernay	Mar. 18 - 19	153
Shandro Injection		
Shandro - Duvernay	Mar. 06 - 07	120
Duvernay - Myrnam	Mar. 07 - 08	124
Myrnam - Elk Point	Mar. 08 - 09	128
Elk Point - Heinsburg	Mar. 09	134
Heinsburg - Lea Park	Mar. 09 - 10	138
Lea Park - Meridian	Mar. 10 - 11	142

3.0 TRAVEL TIME ANALYSIS

3.1 Channel Hydraulics

The North Saskatchewan River between Edmonton and Meridian bridge has an irregular meander pattern with point bars, side bars, mid-channel bars and occasional islands. Hydroelectric power production upstream of Edmonton produces a diurnal fluctuation of about 30% around the mean discharge during the winter. Winter flows also tend to be high because the river is regulated. The river is ice-covered from the middle of November to the middle of April except for a reach between Edmonton and Fort Saskatchewan which is ice free due to thermal effluent discharges from Edmonton.

Ice cover formation on the North Saskatchewan River occurs by a combination of the juxtaposition of ice flows (which includes the redistribution of frazil) and by the consolidation of a juxtaposed cover in locations where the longitudinal forces on an advancing ice cover exceed the strength due to downward freezing of the juxtaposed cover. In the reach between Shandro and Duvernay, this consolidation process resulted in frazil accumulations approaching 2 m in thickness.

Hydraulic characteristics were determined from cross-sections surveyed every five to ten kilometers over the whole reach. These surveys were performed over the month of January by crews from Hamilton and Olsen Surveys Ltd. The ice thickness was found to vary between 0.3 m - 0.8 m while the river top width varied between 120 m and 330 m.

The average times of travel of the leading edge, the peak, the centroid, and the trailing edge of the dye cloud for each subreach are listed in table 3. As well, the cumulative travel times for each test are plotted against distance from injection in figures 2a-b. The slope of the lines in these figures are inversely proportional to the velocities. For example, in both cases the velocity of the peak is about 5% faster than the velocity of the centroid.

Table 3 Subreach average travel times.

Subreach	Length	Travel Times			
		Leading Edge	Peak	Centroid	Trailing Edge
	(km)	(hrs)	(hrs)	(hrs)	(hrs)
Edmonton -Fort Saskatchewan	36.2	14.48	15.50	16.75	21.86
Fort Saskatchewan -Vinca	29.7	11.78	14.50	16.24	29.24
Vinca -Waskatenau	25.6	13.13	13.03	14.17	11.35
Waskatenau -Pakan	28.1	12.41	13.97	14.97	25.62
Pakan -Shandro	27.2	12.50	14.02	14.30	13.56
Shandro -Duvernay	51.3	26.22	28.98	29.12	30.46
Shandro -Duvernay	51.4	26.96	29.00	31.56	40.37
Duvernay -Myrnam	33.2	14.60	18.03	18.18	22.22
Myrnam -Elk Point	25.3	16.27	14.47	16.02	19.74
Elk Point -Heinsburg	33.4	15.89	18.53	18.82	22.17
Heinsburg -Lea Park	18.4	10.10	13.97	12.82	15.53
Lea Park -Meridian	27.9	15.92	14.00	15.93	20.08

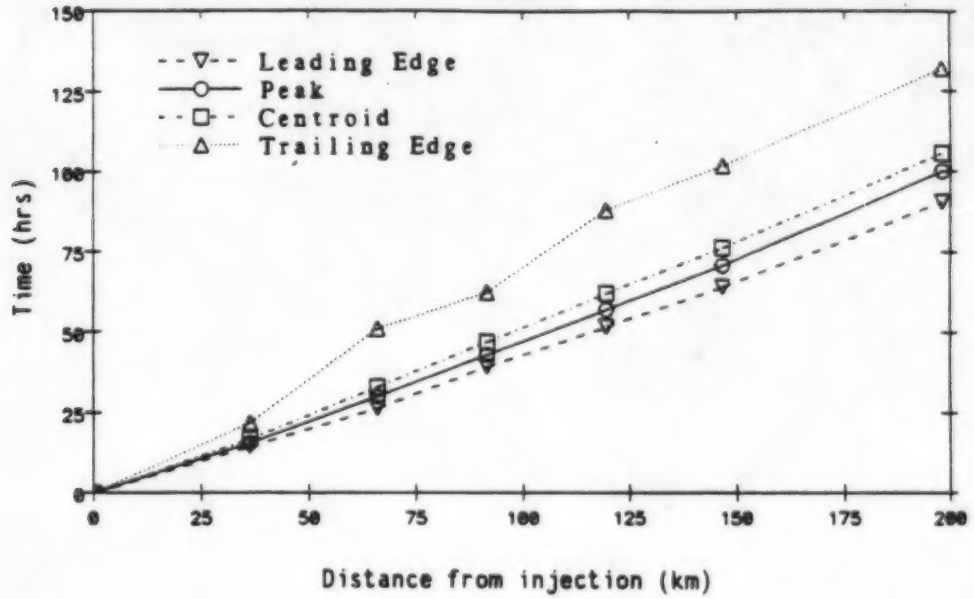

Figure 2a Growth of travel times with distance from injection, Edmonton to Duvernay.

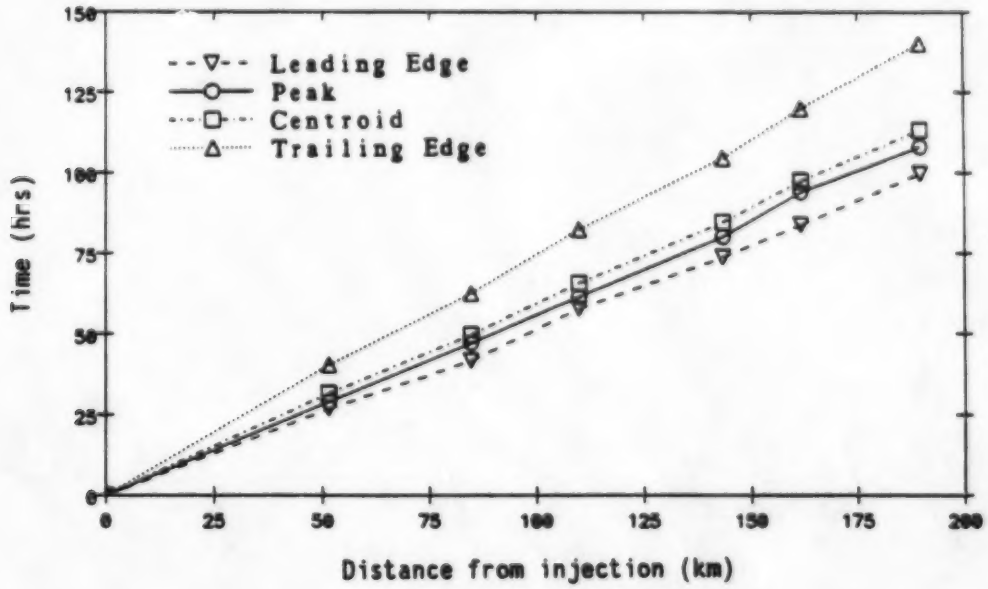

Figure 2b Growth of travel times with distance from injection, Shandro to Meridian.

This difference in velocity between the peak and the centroid of the time-concentration curves raises the question of which quantity represents the average velocity of the water. Obviously, the centroid is the measure of the average velocity of the dye mass but this velocity only corresponds to the average water velocity in a uniform laboratory channel where all areas of the channel contribute to the flow. In natural streams, however, especially for ice-covered winter conditions, the cross-section variability causes zones of stagnant or very slow moving water. These zones contribute little if anything to the discharge therefore they should not be included in the determination of average velocity. The travel time of the centroid of the dye cloud is affected by these stagnant zones especially if they produce long drawn-out receding limbs. Alternatively, the cross-section average velocity of the peak concentration incorporates the cross-sectional variations in velocity but does not include the effects of the storage and release of dye from stagnant areas. Therefore, the velocity of the peak should be used to calculate the hydraulic characteristics of a river reach.

Generalization of the hydraulic characteristics measured at the individual sites into reach-averaged characteristics for each of the subreaches was done by defining the mean velocity, U for each subreach as x/t_p, where x is the reach length and t_p is the time it takes for the peak of the dye cloud to pass through the reach. The resultant subreach mean velocities are given in table 4.

Using the time of travel of the peak to determine the mean velocity may lead to underestimating the time of travel if mixing across the channels not fully established. That is, the dye moves primarily in the zone of high velocity and, hence, the velocity is over estimated because the entire flow is not represented. To estimate the magnitude of this measurement error in the initial subreach, the time of travel between Shandro and Duvernay was measured twice, once at the beginning of a test reach and once at the end of a test reach. Times of travel could not be compared directly because the discharges were not the same for both tests; however, velocities could be compared assuming the channel

Table 4 Summary of average hydraulic characteristics in late winter for each subreach.

Subreach	Reach Length (km)	Velocity (m/s)	Discharge (m^3/s)	Slope	Top Width (m)	Flow Depth (m)	Composite Roughness
Edmonton -Ft. Saskatchewan	36.2	0.65	129	0.000366	172	1.14	0.032*
Ft. Saskatchewan -Vinca	29.7	0.57	108	0.000381	198	0.99	0.022
Vinca -Waskatenau	25.6	0.56	115	0.000443	232	0.90	0.023
Waskatenau -Pakan	28.1	0.56	145	0.000382	145	1.28	0.026
Pakan -Shandro	27.2	0.54	132	0.000397	187	1.30	0.028
Shandro -Duvernay	51.3	0.49	153	0.000359	218	1.43	0.031
Shandro -Duvernay	51.4	0.49	120	0.000359	218	1.12	0.026
Duvernay -Myrnam	33.2	0.51	124	0.000216	210	1.15	0.020
Myrnam -Elk Point	25.3	0.49	128	0.000220	264	1.00	0.019
Elk Point -Heinsburg	33.4	0.50	134	0.000464	212	1.27	0.032
Heinsburg -Lea Park	18.4	0.37	138	0.000232	214	1.74	0.038
Lea Park -Meridian	27.9	0.55	142	0.000179	246	1.01	0.016

* open water reach

roughness remained relatively constant. The velocity in the initial subreach was found to be overestimated by about 9%. The velocity in the initial subreach between Edmonton and Fort Saskatchewan is likely overestimated by less than this value because three, rather than two, injection points were used thereby spreading the dye more quickly over the channel width.

The mean velocity and the adopted discharge, Q were used to determine the flow area, A, for each subreach. From the flow area and top width, the mean depth, d, and the hydraulic radius, A/2W, could be calculated. From these, the composite Manning roughness, n_o, was determined by:

$$[1] \qquad n_o = ((A/2W)^{2/3} AS^{1/2})/Q$$

where S is the average water surface slope. Table 4 summarizes the results.

The composite Manning roughness was found to vary from 0.015 to 0.038. This range of roughness is similar to the open water roughnesses given by Kellerhals, Neill and Bray (1972). This suggests that the underside of the ice cover is very smooth and does not affect the composite roughness significantly. When a similar analysis was done on the Athabasca River between Hinton and Athabasca (Andres, Van Der Vinne, and Trevor, 1989), no significant increase in roughness was observed for low flow winter conditions; however, studies done on the Wapiti and Smoky rivers indicated a significant increase in roughness due to the ice cover in some areas. This difference in the effects of an ice cover on the hydraulic roughness cannot be explained at this time. More effort must be made to quantify the ice cover characteristics if this difference is to be resolved.

3.2 Generalized Travel Times

The travel times for any given discharge are related to the mean velocity of the flow. Because the mean velocity varies monotonically

with discharge in most cases, the measured travel times or velocities are only valid for the discharges at which the measurements were carried out.

The extrapolation to other discharges can be made by combining the equation of continuity:

$$[2] \qquad U = Q/Wd$$

with a roughness equation such as the Manning equation:

$$[3] \qquad Q = (1/n_o)\, R^{2/3}\, W\, d\, S^{1/2}$$

for which all the variables have been defined previously.

It should be noted that for a wide, ice covered channel, the hydraulic radius, R, is given by:

$$[4] \qquad R = A/2W = d/2$$

to account for both the top and bottom boundaries. Combining equations [2], [3], and [4] produces equation [5] which defines the mean velocity in terms of the width, the slope and the composite roughness

$$[5] \qquad U = (Q/2W)^{0.4}\, (S^{0.5}/n_o)^{0.6}$$

Thus for a given river reach, with known values of S, W and n_o, the velocity, and hence the travel time, can be obtained for any given discharge. Figure 3 shows equation [5] in graphical form along with the test results. The curves show the general trend of increasing velocity with increasing discharge for various values of slope and roughness. The data fits equation [5] exactly because a form of the equation was used to calculate the composite roughness.

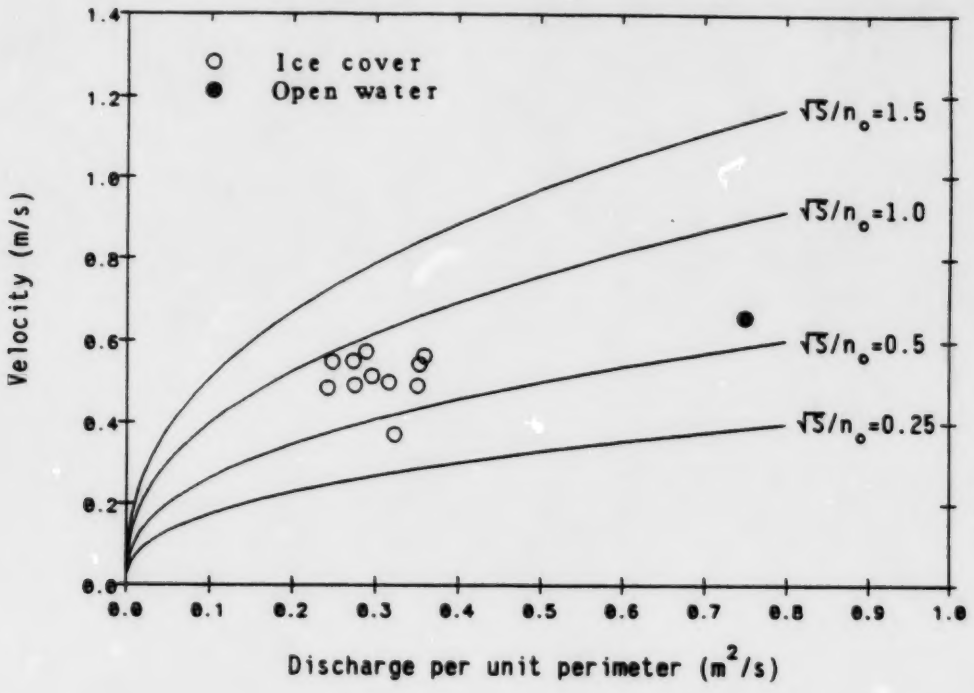

Figure 3 Relationships between mean velocity and discharge per unit width for the North Saskatchewan River under an ice cover.

The above analysis assumes that the composite roughness is constant for all flows, however, it can increase significantly with decreasing discharge as the flow depth decreases in relation to the variations in the channel bottom. If this relationship is approximated by

$$[6] \qquad n_o = a\, Q^{-b}$$

then equation [5] becomes

$$[7] \qquad U = C\, Q^{(0.4+0.6b)}$$

where C is a function of the width and slope of the channel. In some cases, it may be necessary to perform additional travel time measurements at other discharges to define the exponent b. On the North Saskatchewan River, variations in roughness due to changes in discharge

should be minor because the river is regulated. However, large variations in roughness can occur from year to year, depending on the hydrologic and meteorologic conditions. The impact that the ice cover has on the composite roughness is not well understood and therefore it is recommended that the data not be extrapolated too far beyond the conditions for which the measurements were made.

Table 5 Reach-average hydraulic characteristics.

Reach	Discharge (m^3/s)	Slope	Width (m)	Velocity (m/s)	Depth (m)	Shear Velocity (m/s)	Composite Roughness
Edmonton-Duvernay	135	0.000389	196	0.57	1.21	0.048	0.025
Shandro--Meridian	135	0.000294	225	0.49	1.22	0.024	0.025

4.0 DISPERSION ANALYSIS

The tracer dye studies which were done to measure the hydraulic characteristics of the North Saskatchewan River can also be used to measure the rate of longitudinal dispersion, the process by which concentrations are reduced as the pollutant cloud spreads along the length of the channel. This longitudinal dispersion rate can be used to model or predict the extent of toxic concentrations downstream from an accidental chemical spill.

4.1 Reach-average Hydraulic Characteristics

Reach-average hydraulic characteristics are required to determine the nature of longitudinal dispersion in the North Saskatchewan River from the data obtained in the tracer dye tests. Reach-average velocities can be obtained from the slope of the time-to-peak versus distance data for each reach as seen in figure 2. Velocities were quite consistent in both test reaches. Reach-average values of slope and width were calculated from the subreach values given in table 3. Reach-average flow depths were calculated from the average discharge, velocity and widths for each reach. All these hydraulic characteristics are given in table 5.

Table 6 Summary of mixing lengths for single centerline injection.

Reach	Reach Length (km)	Vertical Mixing Length (m)	Transverse Mixing Length (km)	Estimated Linear Mixing Length, α_L=1.0 (km)
Edmonton-Duvernay	198.1	103.6	142	378
Shandro-Meridian	189.5	25.7	182	486

4.2 Mixing Zones

4.2.1 Vertical Mixing

The mixing process in rivers begins as a three-dimensional process but the pollutant concentration quickly becomes uniform over the depth. According to Elhadi et al (1984), vertical variations in concentration are less than 2% at a distance L_v downstream from a source located at mid-depth when

$$[8] \qquad L_v = 1.8\ d\ U/U_* $$

where U_* is the shear velocity defined by

$$[9] \qquad U_* = (gRS)^{1/2}$$

in which g is the acceleration due to gravity.

At Shandro, where the injection was at mid depth, the vertical mixing length was about 26 m (table 6). At Edmonton, however, the injection was near the surface so the mixing length should be four times greater than that given by equation [8], that is, 104 m. Thus, it can be assumed that vertical mixing is instantaneous compared to the total

reach lengths.

4.2.2 Transverse Mixing

Once the pollutant concentration becomes uniform over the depth, the mixing can be treated as a two-dimensional problem. Further downstream, the pollutant concentration becomes essentially uniform over the width of the channel as well. Transverse mixing is essentially complete at a distance L_t from a source located at mid-width when

[10] $$L_t = (0.1U/\epsilon_z)(W)^2$$

(Fischer et al, 1979) where ϵ_z is the transverse mixing coefficient usually estimated from

[11] $$\epsilon_z = k_t d U_*$$

When equations 10 and 11 are combined the result is

[12] $$L_t = (0.1/k_t)\ (U/U_*)\ (W^2/d)$$

Yotsukura and Cobb (1972) introduced a parameter, k_p, which varies with the position of the source in the section and the degree of mixing

[13] $$L_t = 1/(k_p k_t)\ (U/U_*)\ (W^2/d)$$

Values of this position parameter for various fractions of cumulative discharge across a section can be obtained from table 7.

Values of k_t range between 0.4 and 0.8 for natural streams (Fischer et al, 1979); however, these values were measured in open water. Engmann (1974) found that in laboratory channels values of ϵ_z for flows with top covers were only half as large as those for corresponding free surface flows. Engmann proposed that ϵ_z was proportional to the hydraulic radius, R rather than the flow depth, d. Beltaos (1978a), however, measured transverse mixing under ice covers in natural streams

Table 7 Position parameters for various fractions of cumulative discharge across a section and 95% complete mixing.

Fraction of Cumulative Discharge from Nearest Bank	Position Parameter
0.0	3.8
0.1	3.9
0.2	4.5
0.3	5.8
0.4	7.2
0.5	15.7

and found that ϵ_z was more a function of d than R. This conflict has not been resolved so it best to use the field data as a guide rather than the laboratory data. Beltaos (1979) also measured ϵ_z in the North Saskatchewan River without an ice cover and found k_t to be 0.17.

The transverse mixing lengths listed in table 5 were calculated using equation 13 with k_p = 15.7 which corresponds to a single injection in the center of the channel. These lengths define the points where mixing is 95% complete. In the actual tests, however, multiple injections were used to reduce the length required for transverse mixing.

At Shandro, two injections were used, each at one-third of the channel width. This corresponds to 0.2 and 0.6 of the cumulative discharge distribution from the left bank and, from table 7, values for k_p of 4.5 and 7.2 respectively. Transverse mixing lengths for these injections individually are 635 km and 397 km respectively, well beyond the 189.6 km length of the test reach. Complete mixing to the nearest bank from each injection, however, will occur over a much shorter distance. Still, the left bank concentration will be higher than the right bank because the discharge in the left zone was less than that for the right zone. After this point, the only transverse mixing that will occur will be the leveling of the concentrations between the two zones.

To calculate these shorter mixing lengths, it is assumed that the

Table 8 Transverse mixing lengths for multiple injections.

Location	Cumulative Discharge from nearest bank	Position Parameter	Total Transverse Mixing Length (km)	Effective Width (m)	Mixing Length to nearest bank (km)
EDMONTON					
Left side	0.4	7.2	308	160	94
Centerline	0.3	5.8	384	120	53
Right side	0.1	3.9	567	40	5.9
SHANDRO					
Left side	0.2	4.5	635	90	29
Right side	0.4	7.2	396	180	116

injections occur at the center of a streamtube with a width twice the distance from injection point to the nearest bank. For q/Q = 0.2, this width is 2(0.2*225) = 90 m and for q/Q = 0.6, the width is 2(0.4*225) = 180 m. Using these widths and k_p = 15.7 for a centerline injection, the transverse mixing lengths become 29 km and 116 km respectively (table 8). Hence, after 116 km, the river has two completely mixed concentration zones which are slowly equalizing. This can be seen in the measured concentration distributions given in Appendix A. At Elk Point, 110 km downstream of the injection, the right side of the channel still has a significantly lower concentration than the left side. However, at Heinsburg, 143 km downstream of the injection, the concentrations across the channel are much more uniform.

At Edmonton, three injection points dividing the width uniformly were used to reduce the initial concentrations. The discharge distribution at the Edmonton injection site is unknown because the discharge was measured downstream at the Capilano bridge rather than at the injection site. However, the distribution can be estimated assuming that the cross-section is triangular with the deepest point near the

left bank on the outside of the bend and that the local average velocity is directly proportional to the depth. Also, it was observed during the injection that the inside or shallow third of the width was blocked by ice. These assumption result in cumulative discharges of 0.4, 0.7, and 0.9 from the left bank. The transverse mixing lengths for these injections are given in table 8. Total transverse mixing is not completed in the 198.1 km test reach; however, within 100 km the dye is fully mixed to the banks. There is still a small concentration gradient from one bank to the other after this distance but it can be ignored if cross-section average values are used in the analysis.

4.2.3 Linear Dispersion

When transverse mixing is complete, further mixing is due to longitudinal dispersion, the process which increases the spread of pollutant along the channel length as the pollutant travels downstream. Data from a large number of field studies by numerous investigators indicate that the onset of Fickian dispersion is delayed for some distance downstream after transverse mixing is completed (Beltaos, 1978b). In this linear dispersion zone, differential advection and variations in channel geometry cause longitudinal dispersion to occur more quickly than predicted by the Fickian dispersion model discussed in the following section. The field measurements suggest that in this zone the standard deviation, σ_t of the time-concentration distribution grows linearly with distance; hence, this type of dispersion is called 'linear' dispersion.

The location of the transition from linear dispersion to Fickian dispersion can be estimated using

$$[14] \qquad L_L = \alpha_L (U/U_*)(W^2/d)$$

where α_L is a factor varying between 0.48 and 1.8 depending on the degree of channel irregularity. The transition occurs between L_L and $3L_L$. This linear mixing length can be estimated for single injections by assuming that $\alpha_L = 1.0$. Estimated values of L_L are given in table 6

along with the other single injection mixing lengths.

Approximate values of linear mixing lengths for multiple injections can be obtained by assuming each injection stays within its own streamtube. Hence, for two injection points the effective width is one-half of the river width and for three injection points the effective width is one-third of the river width. These multiple injection linear mixing lengths are much shorter than those for single injections because the mixing lengths are proportional to width squared. Using this procedure, the estimated value of L_L for the Edmonton injection is 42 km while for the Shandro injection it is 121 km.

No analytical solution exists for linear dispersion so Beltaos (1978b) proposed the following empirical solution based on the existing data

$$[15] \qquad C = \frac{1}{\sqrt{2\pi\beta}} \frac{MU}{Qx} \left[\frac{Ut}{x} \exp\left[1 - \frac{Ut}{x}\right]\right]^{\frac{1}{\beta}}$$

where β is a parameter defined by

$$[16] \qquad \beta = \left[\frac{\sigma_t}{U/x}\right]^2$$

The calculation of β from measured concentrations can be simplified by defining the pollutant spread in terms of the half-duration, ΔT rather than the standard deviation, σ_t. This eliminates the problems in evaluating σ_t due to incomplete measurements on the falling limb. The half-duration is defined as the period of time during which the concentration is greater than one-half of the peak concentration (figure 4). The half-duration, ΔT of the empirical curve described by equation [15] is equal to 2.36 σ_t; therefore, β can be defined in terms of ΔT

$$[17] \qquad \beta = 0.18\left[\frac{\Delta T}{U/x}\right]^2$$

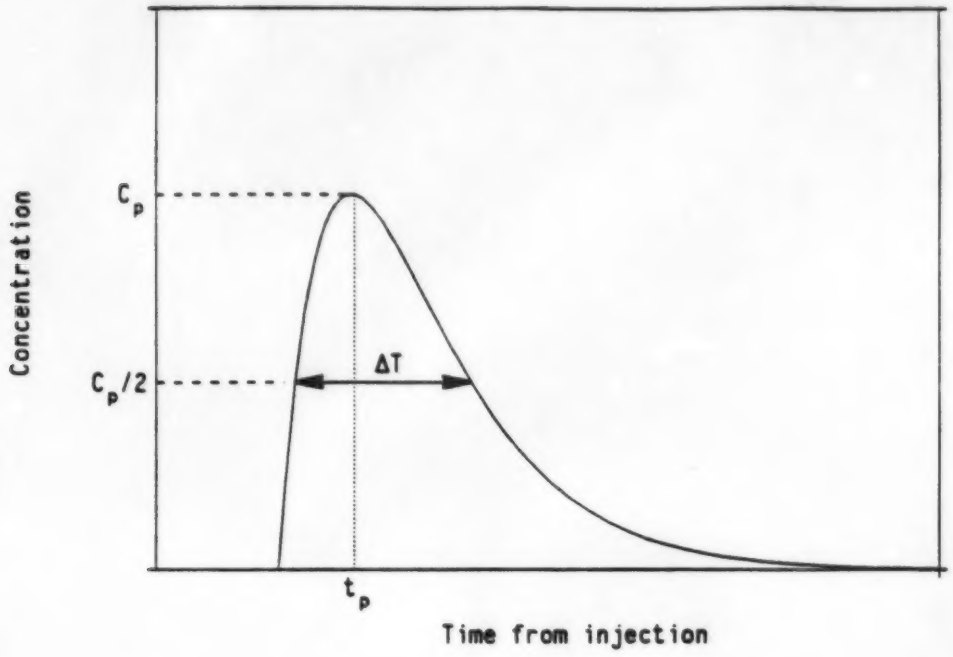

Figure 4 Definition sketch for variables describing time-concentration distributions

4.2.4 Fickian Dispersion

The final mixing process is termed Fickian dispersion. This process can be modeled using the one-dimensional mixing equation

$$[18] \qquad \frac{\delta C}{\delta t} + U\frac{\delta C}{\delta x} = D\frac{\delta^2 C}{\delta x^2}$$

which, for a mass, M instantaneously released throughout a cross-section, has the solution

$$[19] \qquad C = \frac{MU}{2Q\sqrt{\pi Dt}} \exp\left[-\frac{(x-Ut)^2}{4Dt} \right]$$

where C is the cross-sectional average concentration. The properties of this analytical solution indicate that the dispersion coefficient, D can

be defined by

$$[20] \qquad D = \frac{U^3}{2} \frac{d\sigma_t^2}{dx}$$

That is, the rate of change of the variance, σ_t^2 with distance is constant.

4.3 Dispersion Parameters

The dispersion parameters discussed in the previous sections can be evaluated using variables describing the cross-sectional average time-concentration distributions. The variables describing these distributions at each location are: time-to-peak, t_p; half-duration, ΔT; variance, σ_t^2; peak concentration, C_p; and mass recovery ratio, M/M_o. A summary of these variables for each location is given in table 9.

The linear dispersion parameter, β can be evaluated using equation [17], that is, reach-average values of β for the North Saskatchewan River can be obtained from the slopes of the best-fit lines through the half-duration versus time-to-peak data shown in figure 5. Values of β for the two test reaches are listed in table 10. These values of β are lower than values measured in other ice covered rivers; however, they are consistent with the trend of increasing β with U_o/U shown in figure 6 (Beltaos, 1978b). The data shown in this figure also suggests that the presence of an ice cover tends to increase the magnitude of the linear dispersion parameter.

Values of D can also be evaluated from dye test data provided that the test reaches extend into the Fickian range. As stated in equation [20], σ_t^2 vs x is linear in the Fickian range and D is proportional to the slope of this line. Three data points are needed to establish that the trend is linear. The values of D calculated from slopes obtained from figure 7 are given in table 10. There are some significant deviations from the best-fit line for the Edmonton injection, likely due to the lengths of the recession limbs included in the variance

Table 9 Summary of cross-section average time-concentration distribution variables.

Location	Distance from Injection (km)	Time to Peak (hrs)	Half-duration (hrs)	Variance (hrs^2)	Peak Concentration (µg/L)	Mass Recovery Ratio
Edmonton injection						
Ft. Saskatchewan	36.2	15.5	1.79	1.20	6.875	0.750
Vinca	65.9	30.0	6.20	9.56	2.212	0.748
Waskatenau	91.5	43.0	9.26	10.23	1.298	0.756
Pakan	119.6	57.0	11.34	29.94	1.127	0.849
Shandro	146.8	71.0	13.39	32.47	0.902	0.824
Duvernay	198.1	100.0	17.12	45.83	0.676	0.832
Shandro injection						
Duvernay	51.4	29.0	4.95	4.61	4.973	0.783
Myrnam	84.6	47.0	8.08	7.77	3.584	0.934
Elk Point	109.9	61.5	9.39	16.33	2.843	0.899
Heinsburg	143.3	80.0	13.16	27.13	2.085	0.922
Lea Park	161.7	94.0	14.98	37.75	1.811	0.953
Meridian	189.6	108.0	15.24	47.38	1.753	0.966

Table 10 Summary of dispersion parameters.

Reach	Linear Dispersion Parameter β	Linear Mixing Length L_L (km)	Linear Mixing Length Factor α_L	Fickian Dispersion Coefficient D (m^2/s)
Edmonton-Duvernay	0.00612	34.6	0.83	344
Shandro-Meridian	0.00429	66.4	0.55	291

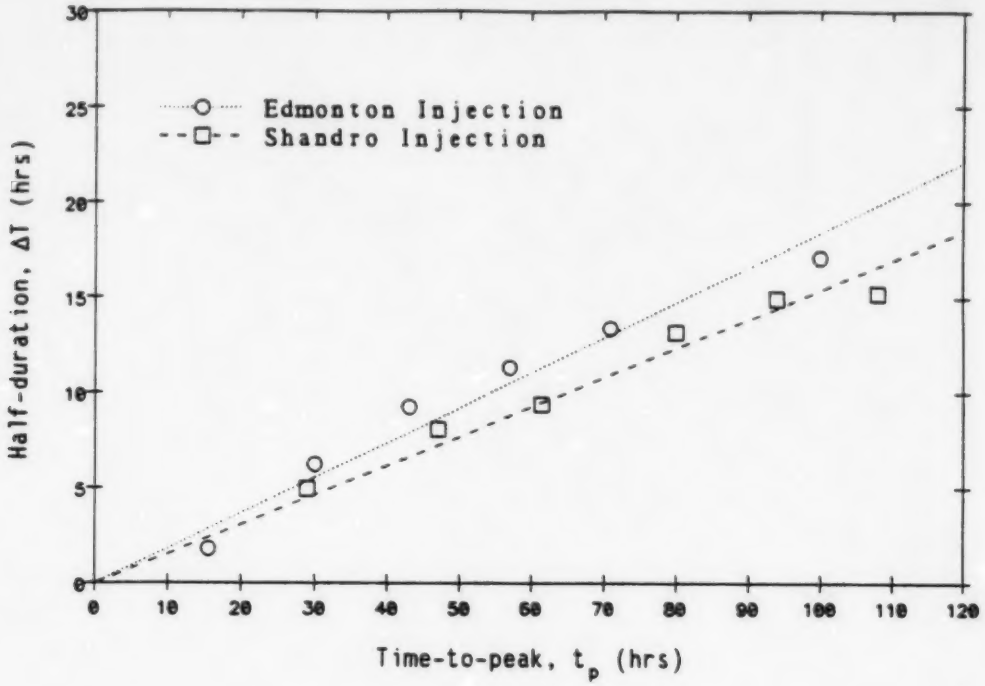

Figure 5 Variation of half-duration with time-to-peak from injection.

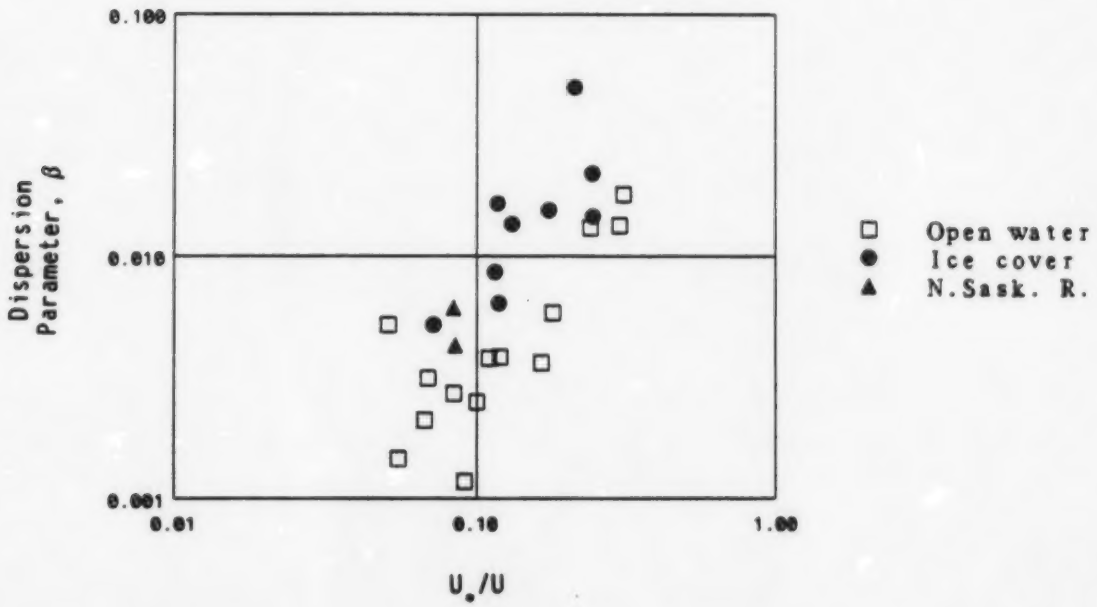

Figure 6 Variation of β for both open water and ice covered conditions (Beltaos, 1978b).

calculations. The dispersion coefficients measured in this study are consistent with values reported in the literature for channels of this width and roughness (figure 8). Not enough of these measurements have been done under an ice cover to make any conclusions regarding the effects of an ice cover on the dispersion coefficient.

Actual values, or at least lower limits, of L_L can also be obtained from figure 7. Beltaos (1978b) defined L_L as the x-intercept of a straight line fitted through the σ_t^2 vs x data in the Fickian dispersion zone. Once L_L is evaluated, the actual value of α_L can be obtained from equation [14]. Values of both L_L and α_L for the test reaches are given in table 10. The three injection points at Edmonton cause Fickian dispersion to begin much more quickly in the upper test reach. In the lower reach, the reach length was slightly less than $3L_L$ away from the injection site so Fickian dispersion did not occur.

The values of L_L given in table 10 are similar to the values estimated in section 4.2.3 but are less than the transverse mixing lengths given in table 8 because L_L is evaluated from cross-section average values. Thus, only average concentrations can be predicted before transverse mixing is complete.

4.4 Dispersion Model Predictions

4.4.1 Linear Dispersion

Time-concentration distributions were generated for each sample site using the linear dispersion model defined in equation [15]. These predicted distributions are plotted in figure 9 along with the cross-section average of the measured distributions. The major discrepancy between the measurements and the model predictions is in the magnitude of the peak concentrations. The model predicts peak concentrations as much as 50% higher than the measured values.

An assumption in the model is that the dye is completely conserved but the mass recovery ratios plotted in figure 10 show that as much as

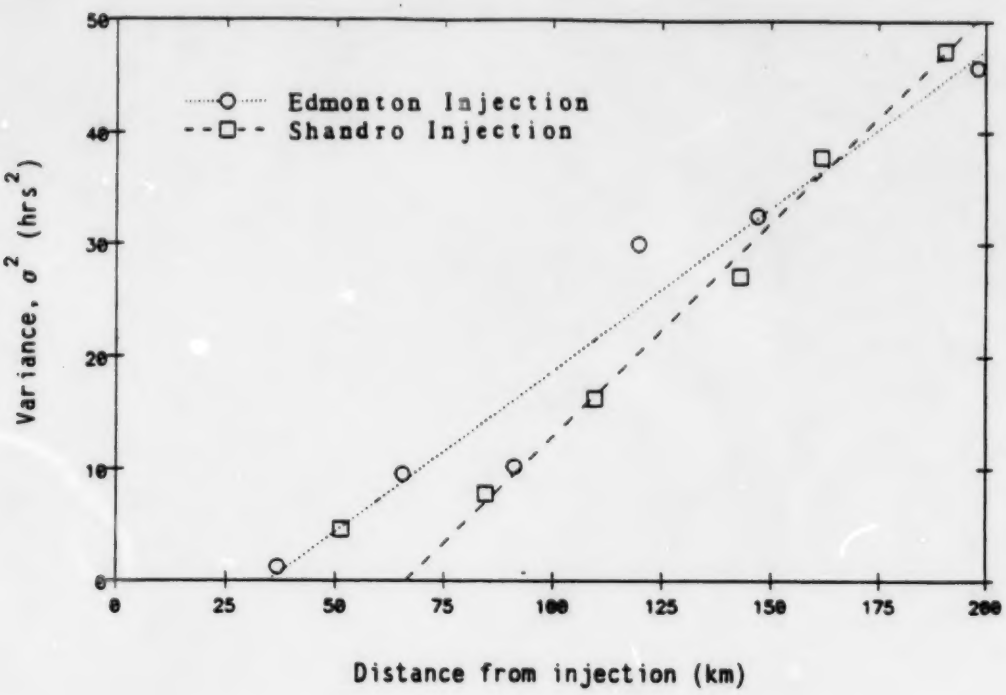

Figure 7 Increase in variance with distance from injection.

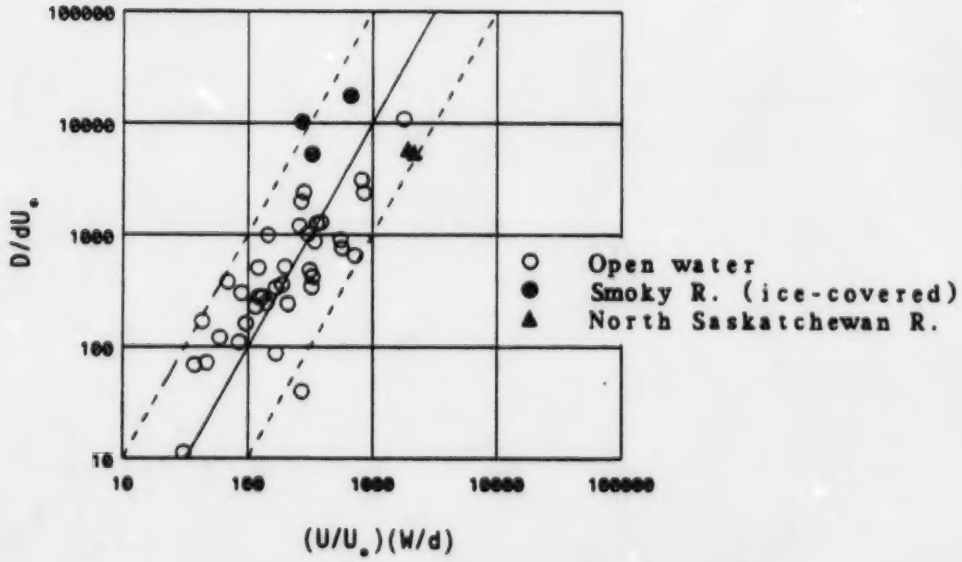

Figure 8 Variation of dimensionless dispersion coefficient (Beltaos, 1978b).

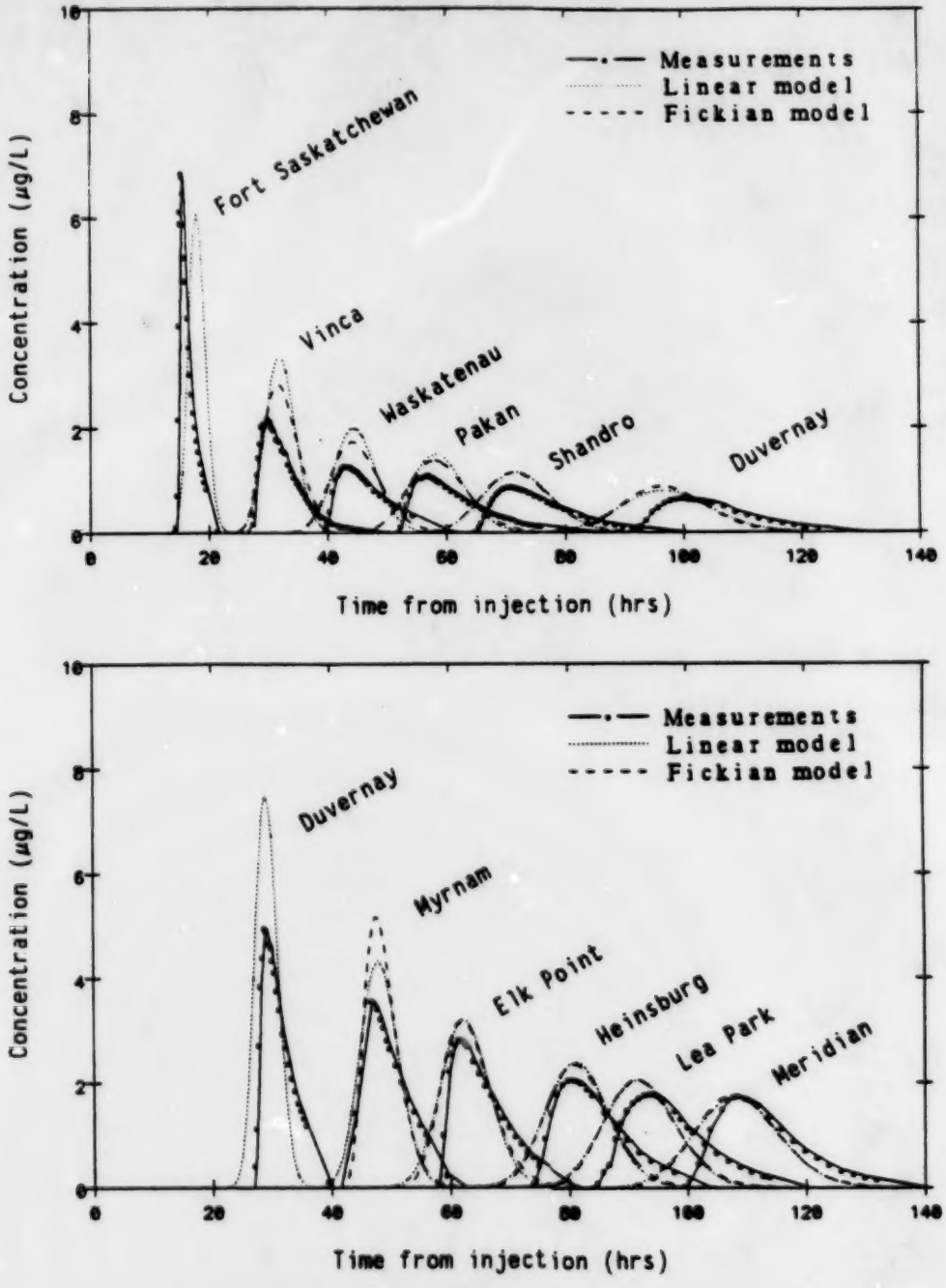

Figure 9 Comparison of measured time-concentration distributions with those predicted by the linear dispersion model.

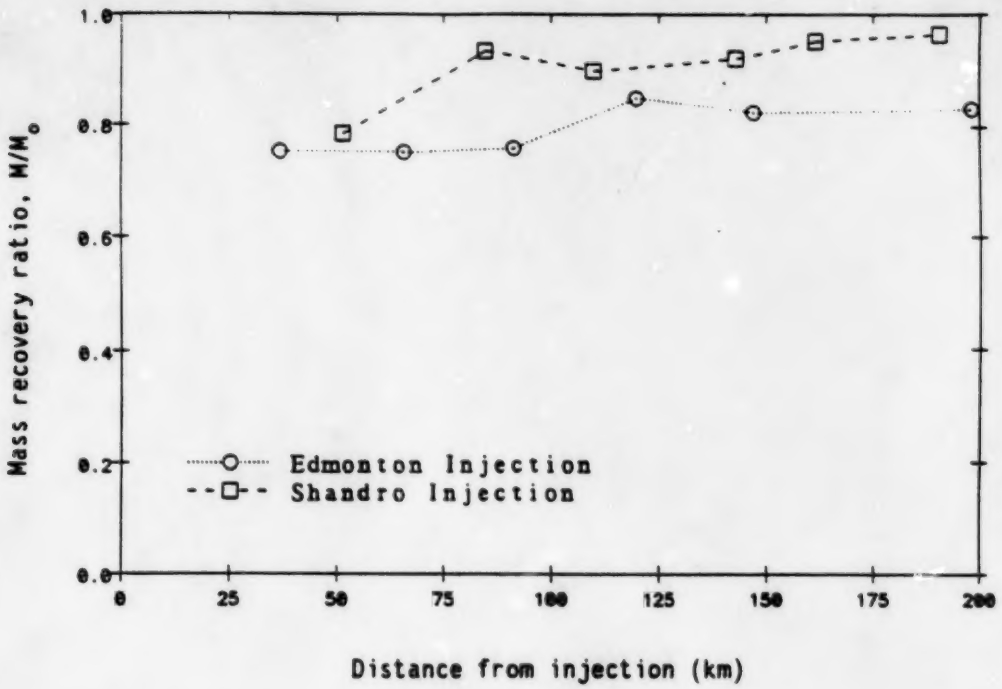

Figure 10 Variation in mass recovery ratio with distance from injection.

25% of the dye was undetected at some of the sample sites. This undetected dye may be lost due to chemical and physical processes or it may be due to inaccurate assumptions of discharge or water temperature. For example, the increase in mass recovery ratio between Fort Saskatchewan and Pakan is likely because water temperatures in the open water reach were greater than the assumed near freezing value. If the model were modified to account for losses in mass, the predicted time-concentration distributions would match the measurements much more closely.

The peak concentrations predicted by the model may also be higher than the measured peaks because of the difference in shape between of the predicted and measured time-concentration distributions shown in figure 9. The more symmetrical curves predicted by the model have shorter durations, therefore the peaks would be higher even if the dye masses were the same. The model could be improved by making it predict

the shape of the time-concentration distributions more accurately.

The times-to-peak of the predicted distributions are slightly different from the measured values as well. This difference is caused by the model using reach-average velocities rather than measured sub-reach velocities.

The model predictions are reasonable considering all the assumptions and approximations used to obtain the modeling parameters. The linear dispersion model can be used with confidence to predict concentrations downstream of accidental releases of pollutants as long as some margin for error is incorporated into the results. However, this model should only be used until the point where Fickian dispersion begins.

4.4.2 Fickian Dispersion

Elhadi et al (1984) state that once a pollutant cloud passes a point $3L_L$ away from the spill site, equation [10] should be used to predict concentrations. Equation [14] can be used to estimate L_L for single injections; however, this distance is so large for the North Saskatchewan River that Fickian dispersion would not occur until well into Saskatchewan.

In the case of the multiple injection tests done in this study, L_L can be estimated by dividing the channel width by the number of injections and using this reduced width in equation [14]. As well, Equation [19] cannot be used as it stands because its derivation assumed complete mixing across the section immediately upon injection. To make equation [19] suitable for modeling dispersion from sources other than completely mixed sources, it must be assumed that the pollutant is injected, fully mixed, at a virtual origin a distance L_L downstream from the actual injection. Thus equation [19] becomes

$$[21] \qquad C = \frac{MU}{2Q\sqrt{\pi D(t-t_o)}} \exp\left[- \frac{(x-U(t-t_o))^2}{4D(t-t_o)} \right]$$

where t_o is defined as L_L/U.

Predicted distributions using this modified Fickian dispersion model are shown in figure 9 along with those of the linear model. All locations greater than L_L were modeled to show the inaccuracy of the model in the linear dispersion zone. Note that the peaks predicted by the Fickian dispersion model are highest at both Vinca and Myrnam; however, by the end of the reaches, predictions from the two model are quite similar. If the reaches were extended, the linear model would begin to overpredict dispersion while the Fickian model would be more accurate.

4.0 SUMMARY

Two tracer dye tests were carried out on the North Saskatchewan River between Edmonton and the Saskatchewan border. Discharges during the tests ranged from 108 m^3/s to 153 m^3/s. Ice thicknesses varied between 0.3 m and 0.8 m with frazil accumulations approaching 2 m in some places. Velocities calculated from the travel times of the peak concentration ranged between 0.37 m/s and 0.57 m/s in the ice-covered reaches. Composite hydraulic roughnesses varied between 0.016 and 0.038. The extrapolation of these velocities is possible, provided some confidence can be placed on the adopted values of hydraulic roughness for the extrapolated conditions. Because the roughness depends significantly on the ice conditions, which in turn can vary substantially from year to year and throughout the winter season, it is recommended that care be taken to verify the characteristics of the ice cover prior to extensive extrapolations.

Two types of longitudinal dispersion occurred during the dye tests. First, after transverse mixing was completed, 'linear' dispersion occurred, where the length of the dye cloud grew linearly with distance. After a transition period, the second type of longitudinal dispersion, Fickian dispersion, began where the length grew with the square root of distance.

The linear dispersion parameter was found to be 0.00612 for the Edmonton injection and 0.0429 for the Shandro injection. These values are lower than the values measured on other ice covered rivers but this is due to the low values of hydraulic roughness found in these river reaches. The Fickian dispersion coefficient was found to be 344 m^2/s for the upper reach and 291 m^2/s for the lower reach. These values are consistent with values reported in the literature for channels of similar width and roughness even with the presence of an ice cover.

Once the loss of dye was taken into account, the major discrepancy between the results of the longitudinal dispersion models and the measurements was the shape of the concentration distributions. The models predicted much more symmetrical distributions than were actually

observed.

The analysis of the data presented herein provided some information on both the hydraulic and mixing characteristics on the North Saskatchewan River; but, further information is required to gain a more complete understanding of these characteristics. To gather this information, it is recommended that:

(1) a low flow open water travel time test be undertaken to better quantify the low flow open water hydraulic and mixing characteristics and

(2) a study be undertaken to quantify the variations in length of the open water reach downstream of Edmonton over winter to determine the impact of this variation on the hydraulic and mixing characteristics.

5.0 REFERENCES

Andres, D, Van Der Vinne, G., and Trevor, B. (1989): Low flow winter travel time characteristics of the Athabasca River, Hinton to Athabasca. Surface Water Engineering Report No. SWE-89/06. Resource Technologies Department, Alberta Research Council.

Beltaos, S. (1978a): Transverse mixing in natural streams. Transportation and Surface Water Engineering Division Report No. SWE-78/01, Alberta Research Council.

Beltaos, S. (1978b): An interpretation of longitudinal dispersion data in rivers. Transportation and Surface Water Engineering Division Report No. SWE-78/03, Alberta Research Council.

Beltaos, S., Anderson, M.D. (1979): Mixing characteristics of the North Saskatchewan River below Edmonton, Part I. Transportation and Surface Water Engineering Division Report No. SWE-79/01, Alberta Research Council.

Engmann, E.O. (1974): Transverse mixing characteristics of open and ice-covered channel flows. Ph.D. thesis, Department of Civil Engineering, University of Alberta, Edmonton, Alberta.

Elhadi, N., Harrington, A., Hill, I., Lau, Y.L., and Krishnappan, B.G. (1984): River mixing - a state-of-the-art report. Canadian Journal of Civil Engineering, Vol. 11, No, 3, pp. 585-609.

Fischer, H.B., List, E.J., Koh, R.C., Berger, G.N., and Brooks, N.H. (1979): Mixing in inland and coastal waters. Academic Press, N.Y.

Kellerhals, R., Neill, C.R., and Bray, D.I., (1972): Hydraulic and geomorphic characteristics of rivers in Alberta. River Engineering and surface Hydrology Report No. 72-1, Alberta Research Council.

Yotsukura, N. and Cobb, E.D., (1972): Transverse diffusion of solutes in natural streams. USGS Prof. Paper 582C.

APPENDIX A

Dye Concentration Measurements

Ft. Saskatchewan sample site
downstream side of Hwy 15 bridge

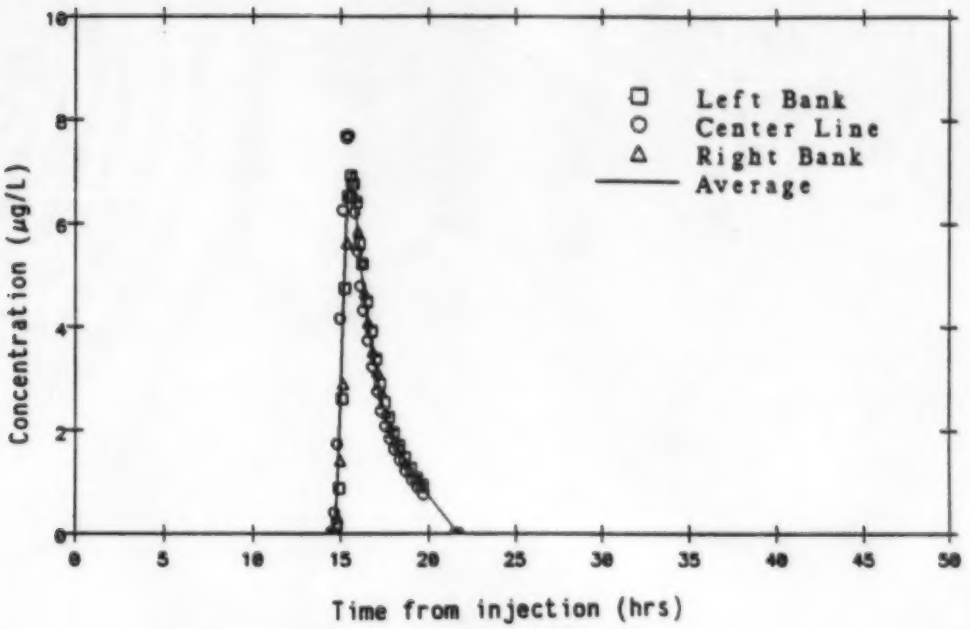

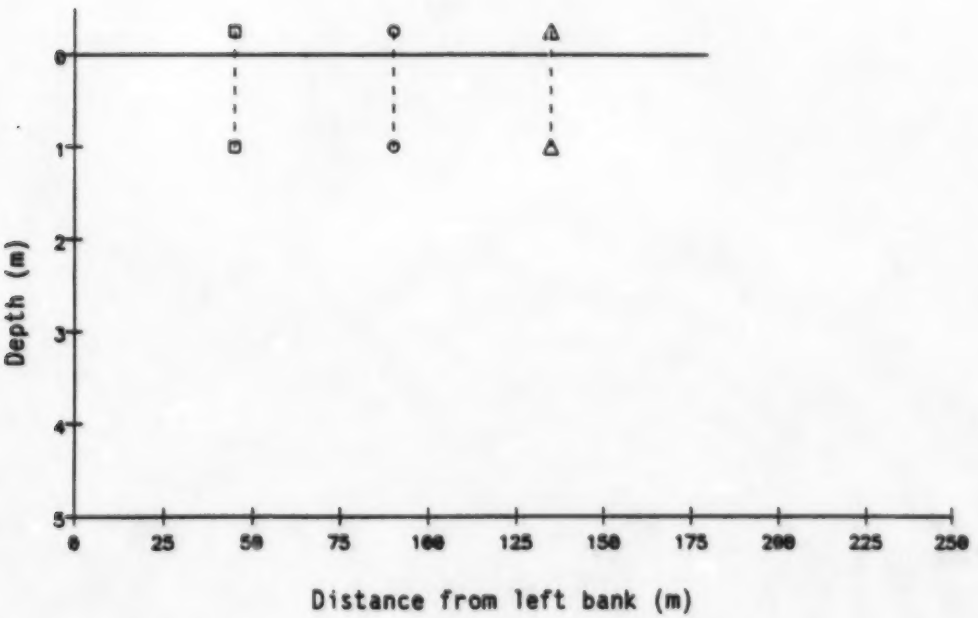

Vinca sample site
33m upstream of Hwy 38 bridge

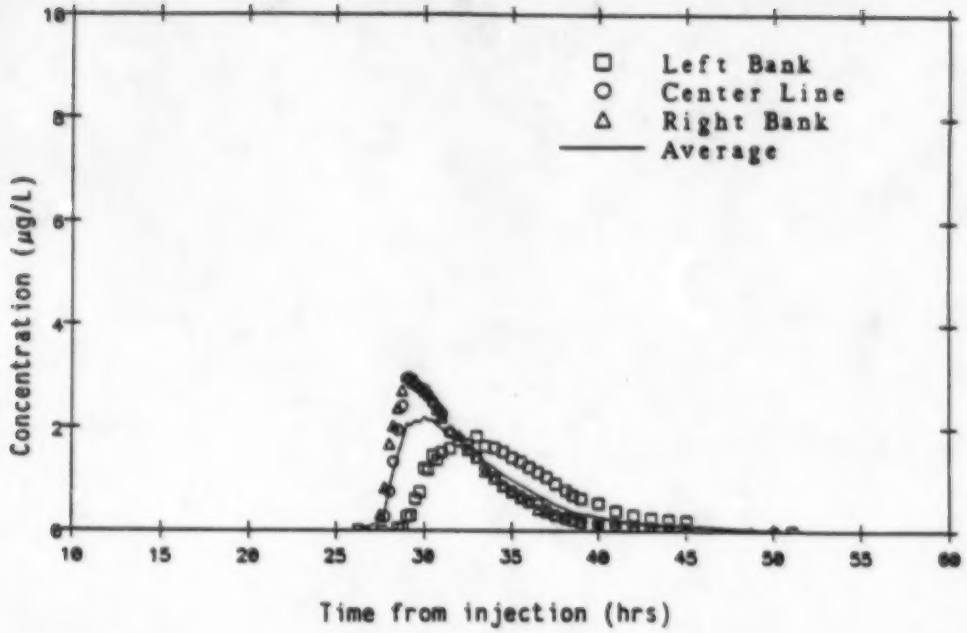

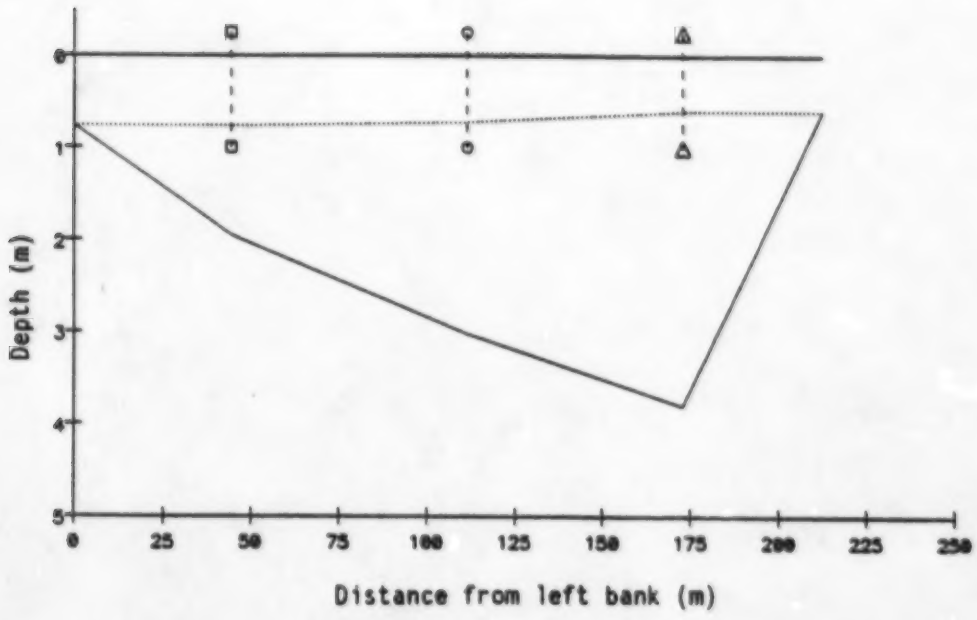

Waskatenau sample site
200m upstream of Hwy 831 bridge

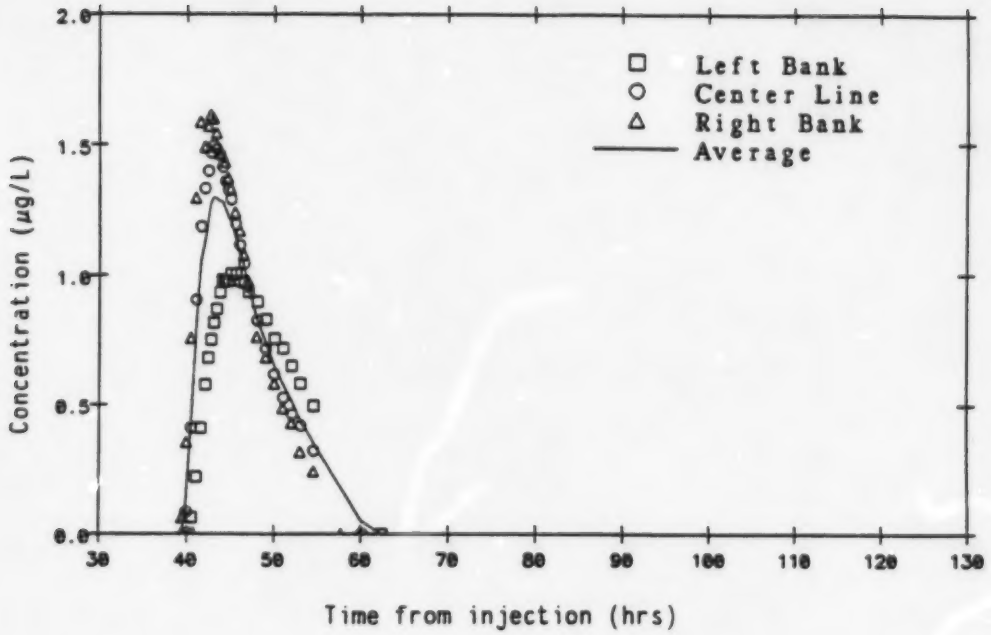

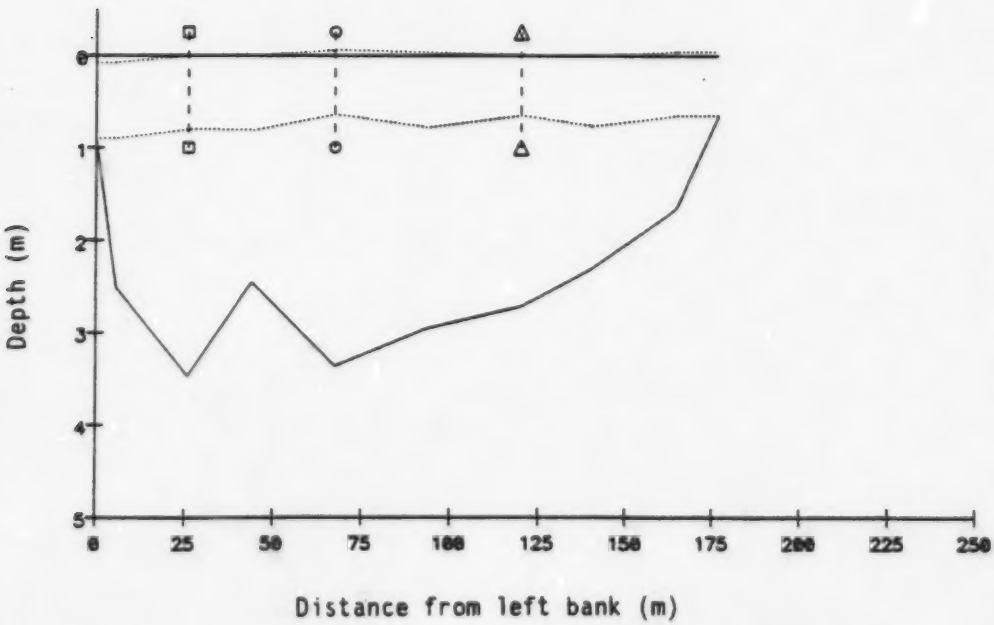

Pakan sample site
30m downstream of old ferry access

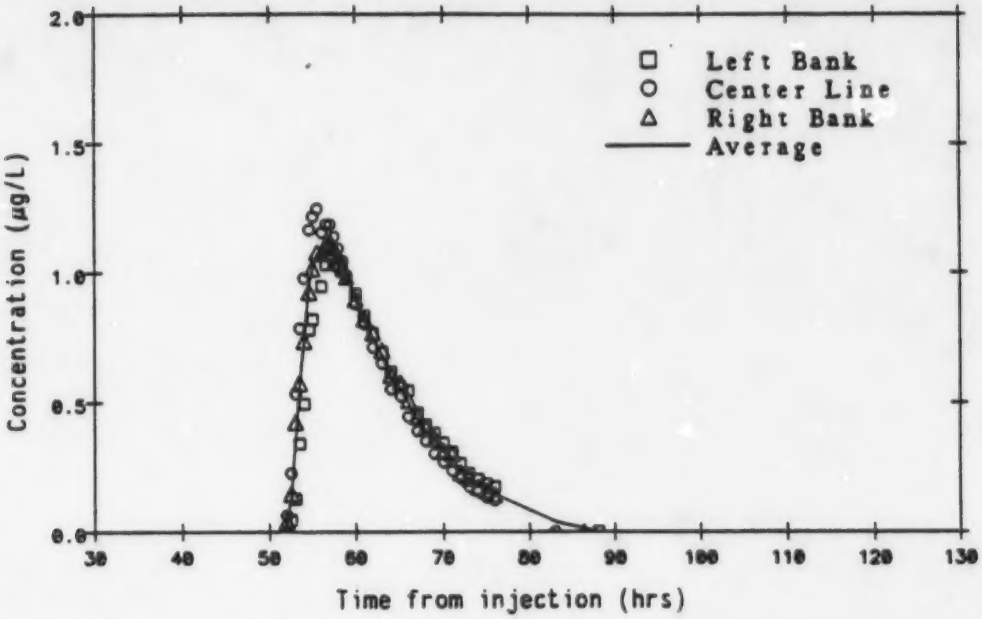

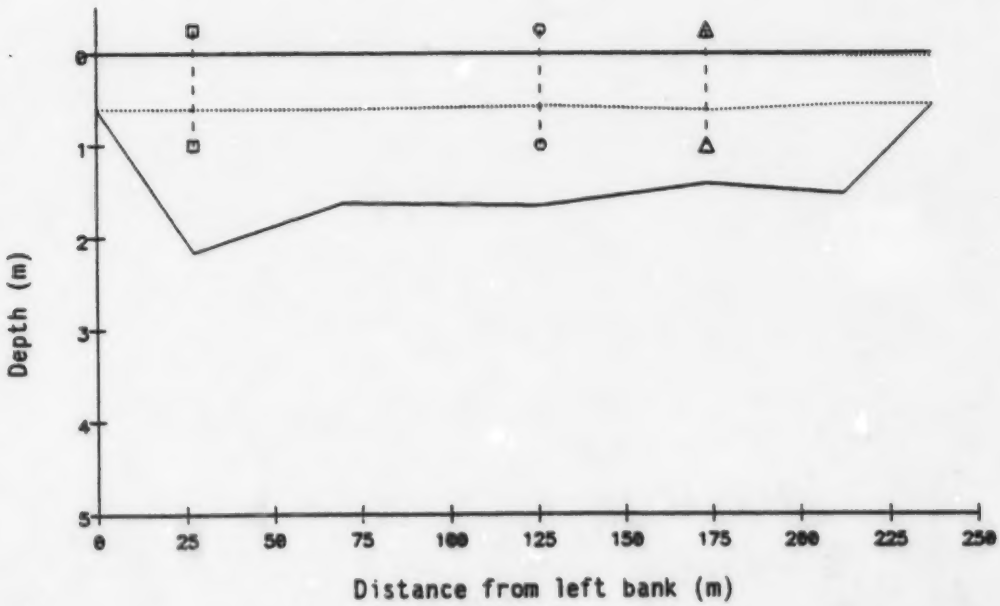

Shandro sample site
200m downstream of Hwy 857 bridge

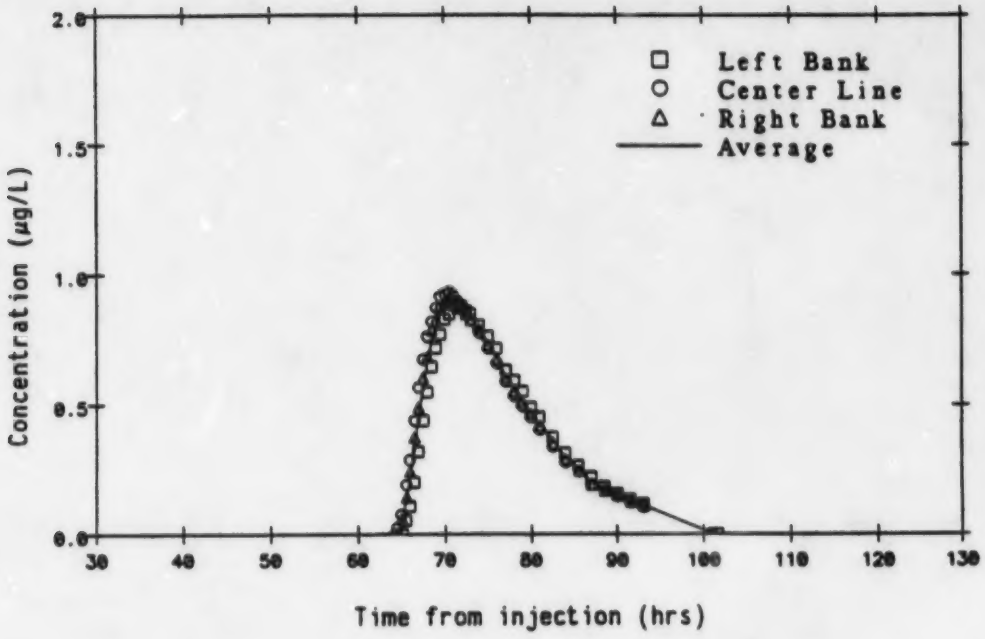

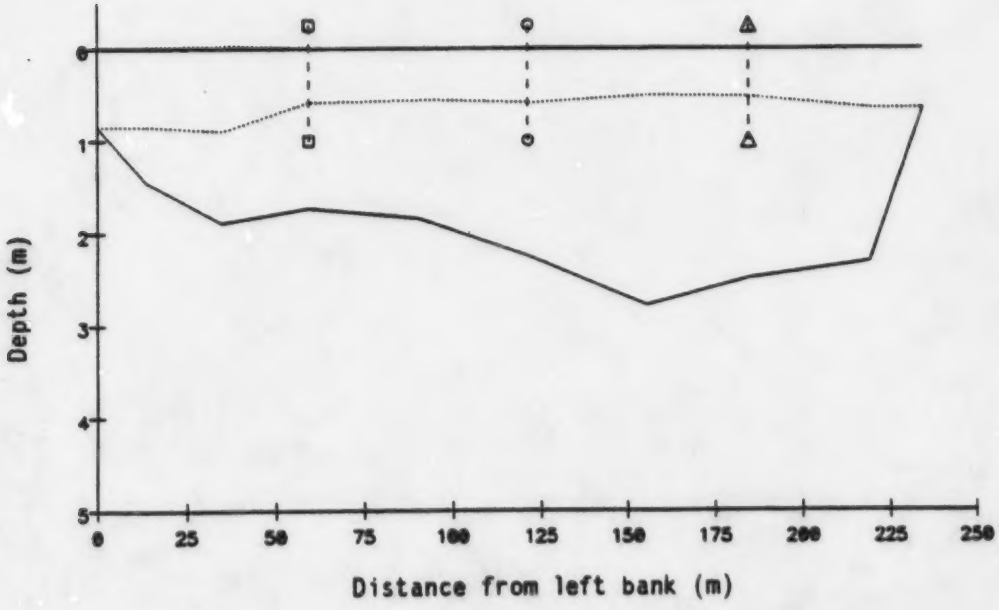

Duvernay sample site
2.315km downstream of Hwy 36 bridge

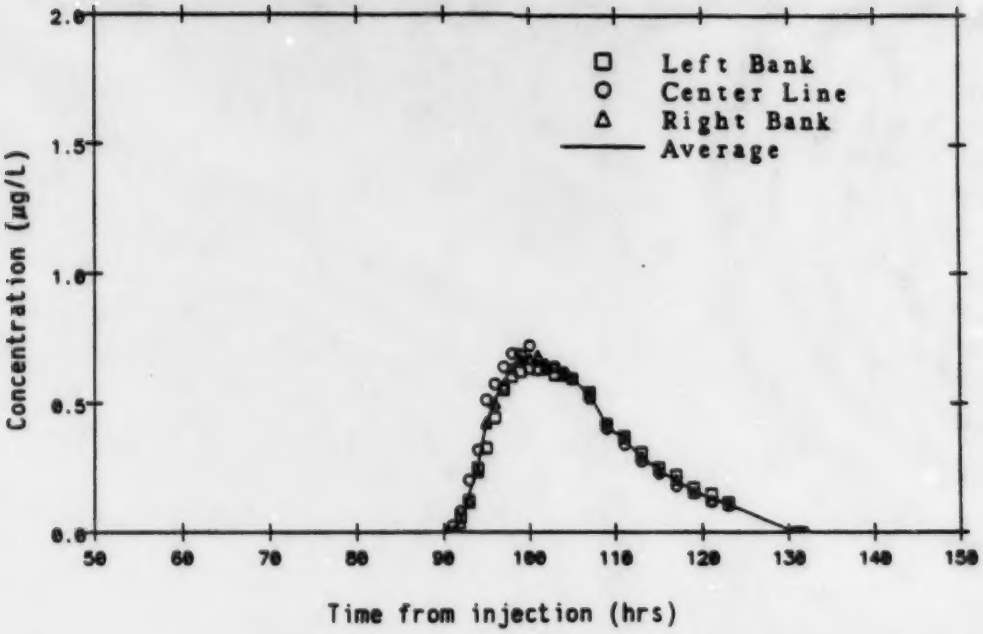

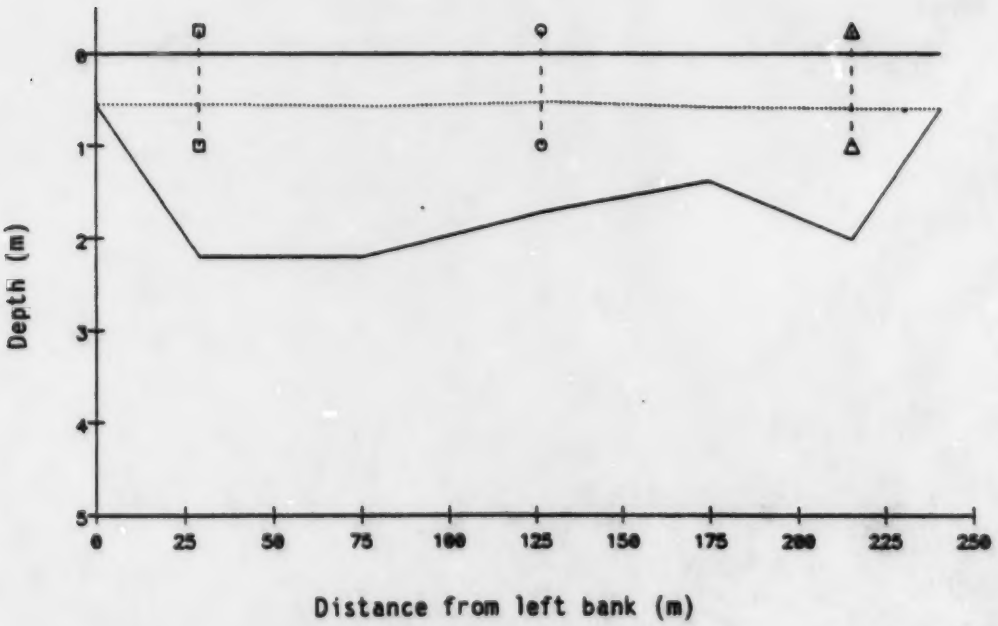

Duvernay sample site
2.315km downstream of Hwy 36 bridge

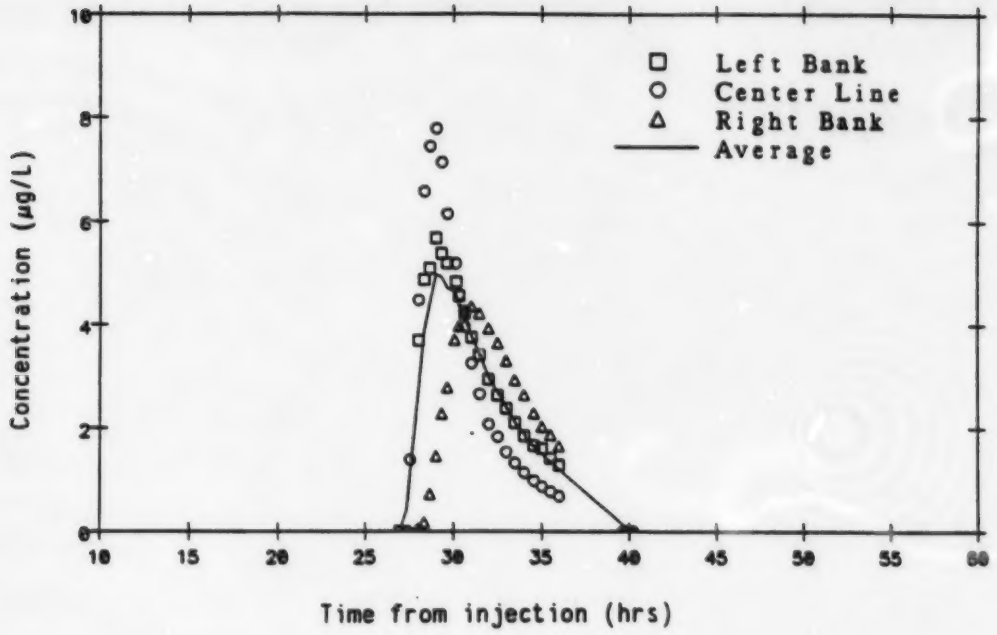

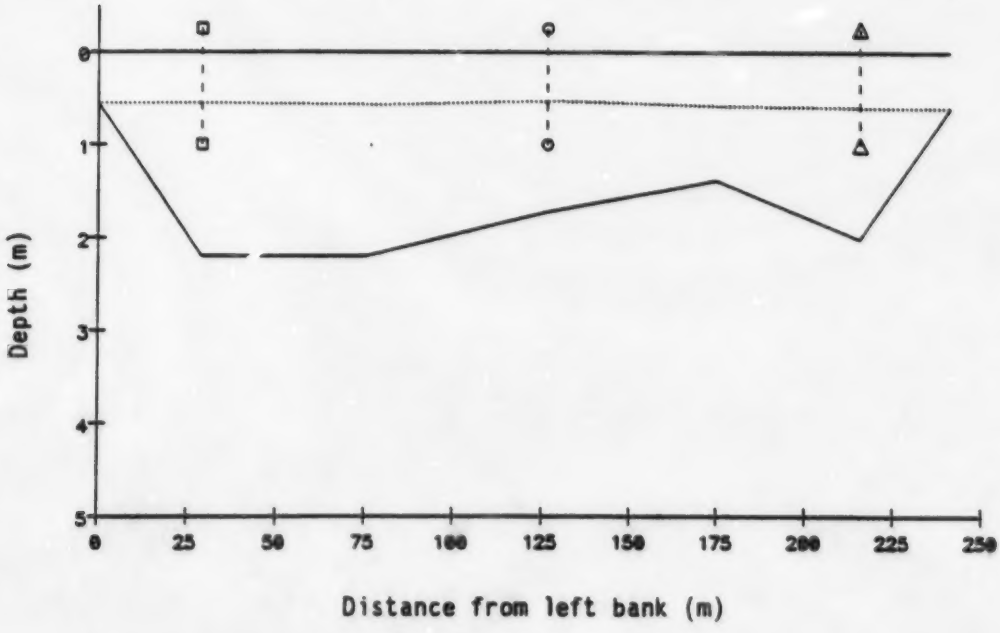

Myrnam sample site
at old ferry access 620m downstream of Hwy 881 brigde

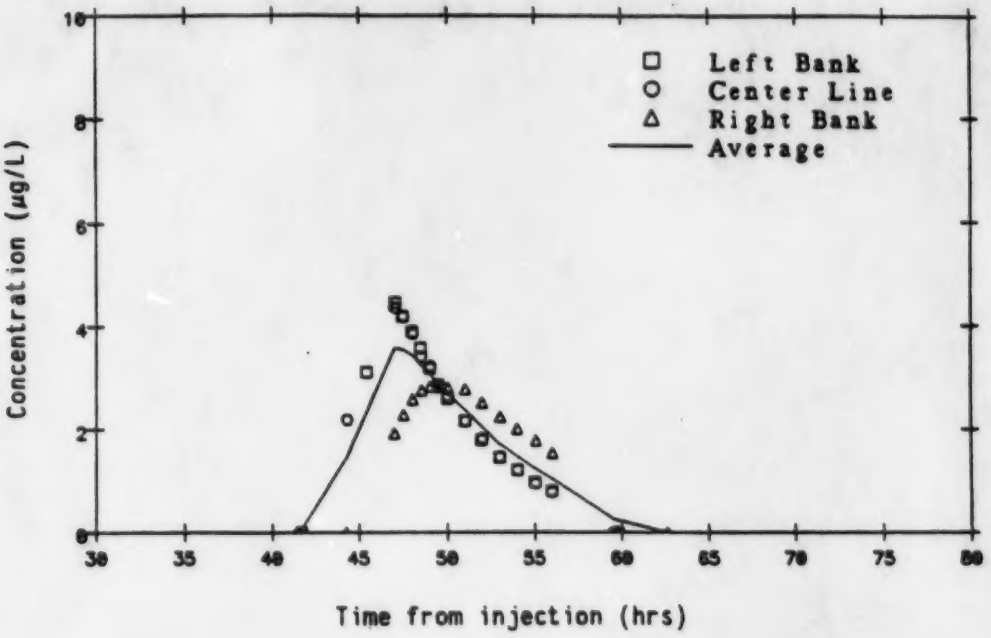

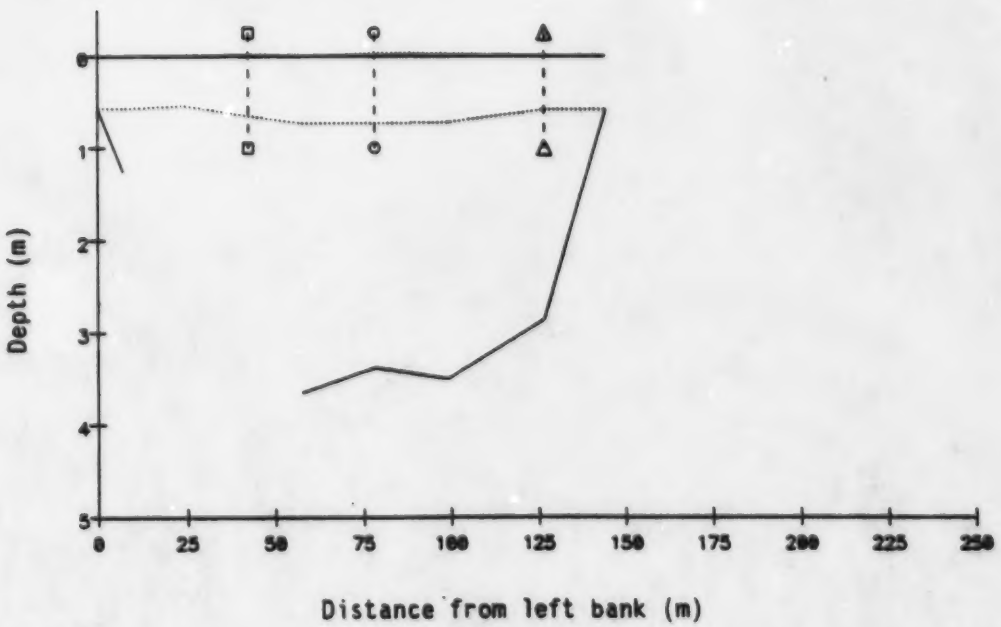

Elk Point sample site
125m upstream of Hwy 41 bridge

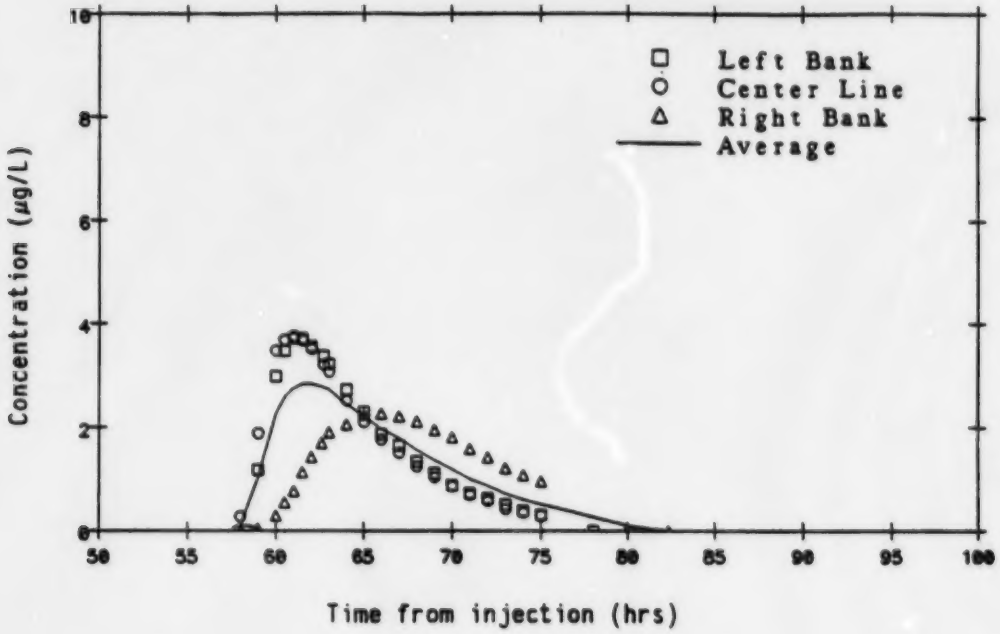

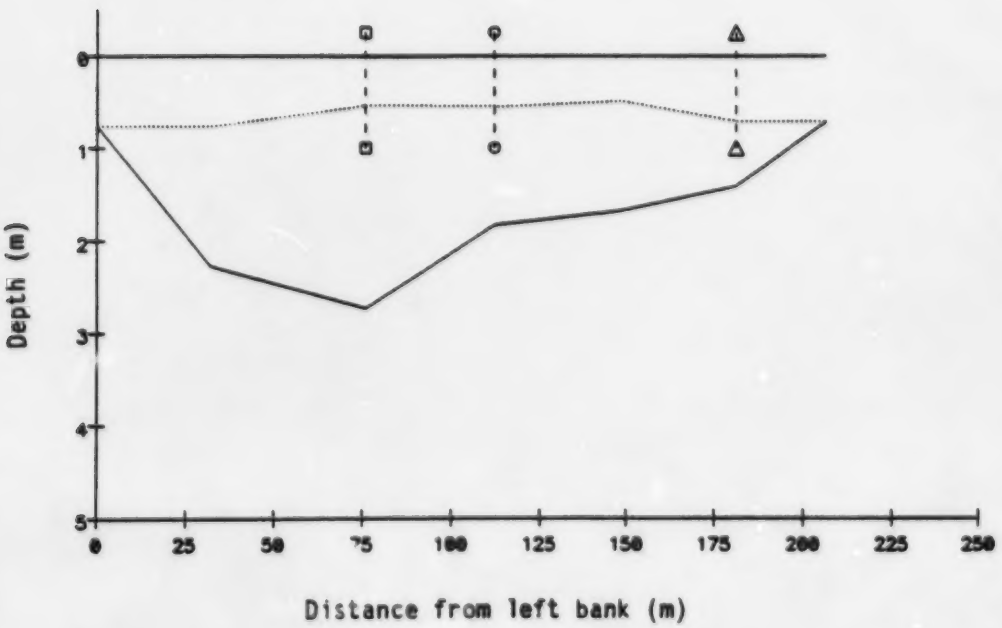

Heinsburg sample site
750m downstream of Hwy 893 bridge

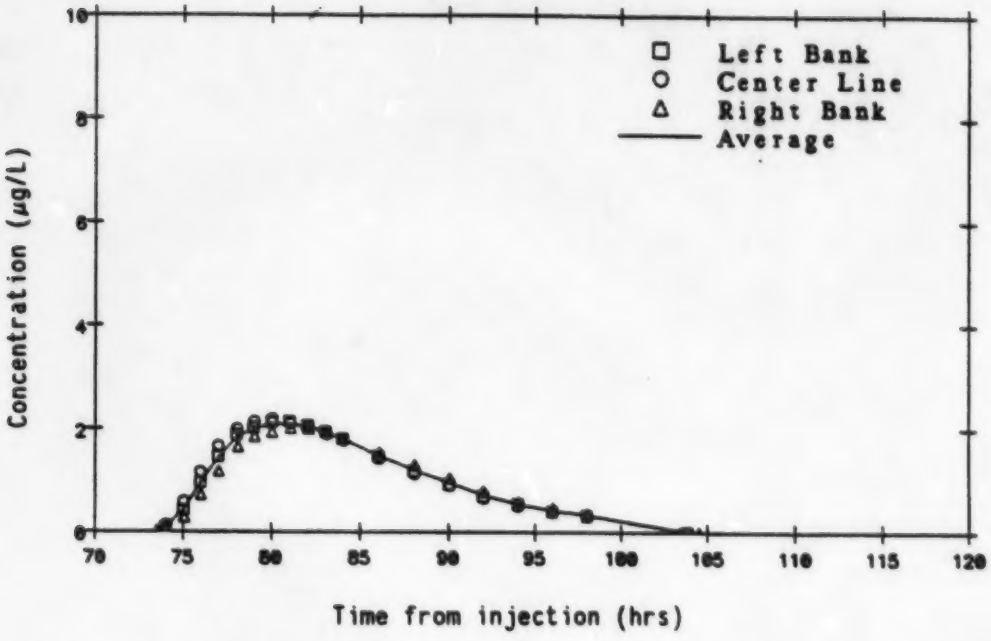

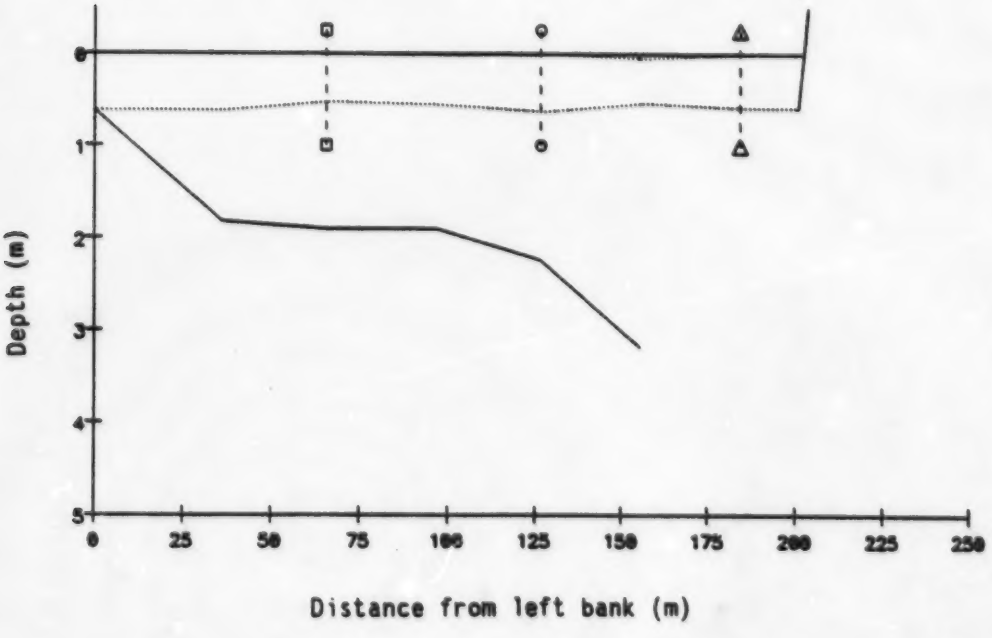

Lea Park sample site
30m upstream of Hwy 897 bridge

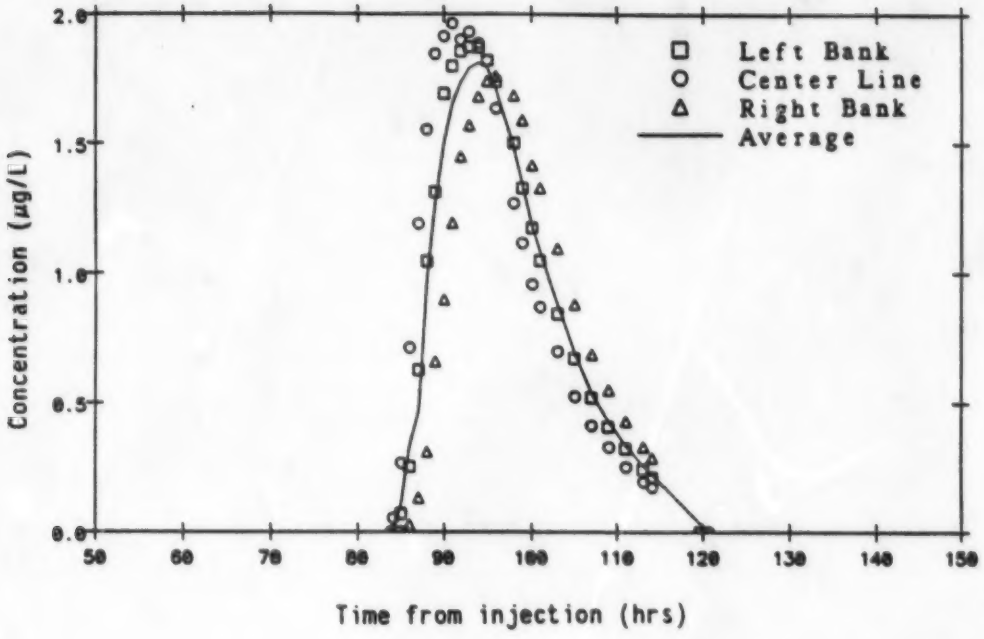

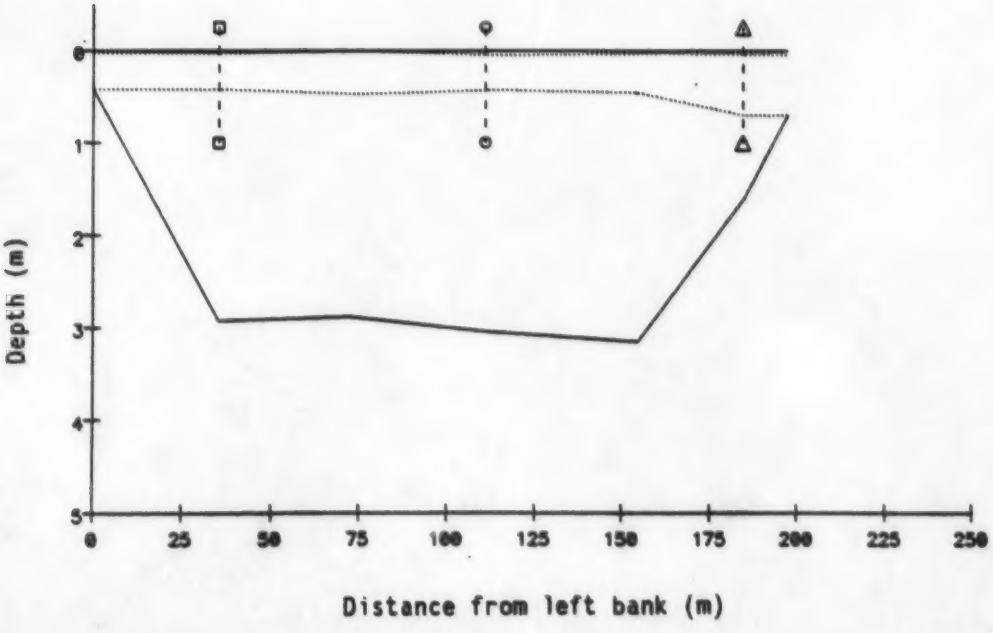

Meridian sample site
30m downstream of Hwy 17 bridge